



UNIVERSITAT DE
BARCELONA

Bachelors Thesis

Electronic Engineering of Telecommunications

Faculty of Physics

Radar System Design based on
Frequency-Modulated Continous Wave
transmission.

Barcelona, (February 9, 2020)

Autor: Òscar Romeu Tello

Director: Javier Jose Sieiro Cordoba

Contents

1. Introduction	1
1.1. Main aim and scope of the project	1
1.2. Target audience	2
1.3. Methodology	2
1.4. Facilities	2
1.5. Bachelor thesis outline	2
2. Radar systems overview	5
2.1. Radar principle	5
2.2. Radar Equation and System Considerations	5
2.3. Modulation Patterns	8
2.4. Doppler Effect and () Radar	9
2.5. () Radar	11
2.5.1. Stationary-Target Case	11
2.5.2. Moving-Target Case	13
2.6. Receiver Architectures	14
2.6.1. Homodyne	14
2.6.2. Single-Conversion Superheterodyne Receiver	15
2.7. Spectrum regulation	16
3. Background and related work	17
3.1. Historical background	17
3.2. Previous work	17
4. Requirements analysis	21
4.1. Architecture selection	21
4.2. Description of the modules	21
4.2.1. Transmission elements	21
4.2.2. Receiver elements	22
4.3. PCB Materials	23
4.3.1. Wilkinson	23
4.3.2. Antenna selection	23
5. Detailed design of the Radar	25
5.1. Radar System Analysis	25
5.2. VCO	26
5.3. Amplifier	26

5.4.	Wilkinson	28
5.4.1.	Introduction	28
5.4.2.	Design procedure	29
5.4.3.	Experimental Results	29
5.5.	Vivaldi Design	30
5.5.1.	Introduction	30
5.5.2.	Antenna design and configuration	30
5.5.3.	Simulation results and discussion	32
5.5.4.	Experimental results	33
5.6.	Radar Results	34
5.7.	Radar Revisited	36
6.	Feasibility study of the project	37
6.1.	Execution planning	37
6.2.	Economical aspects	40
7.	Conclusions and future work	41
	Bibliography	43
A.	Datasheets	45
A.1.	Mixer	45
A.2.	Voltage Controlled Oscillator	46
A.3.	Power Amplifier	46
A.4.	Low Noise Amplifier	47
B.	Schematics	49

List of Figures

2.1. Basic radar system.	6
2.2. Typical modulation patterns.	9
2.3. Target moving at an angle θ	10
2.4. Basic block diagram of CW RADAR.	10
2.5. Basic block diagram of FMCW RADAR.	11
2.6. Basic block diagram of FMCW RADAR.	12
2.7. Range and relative velocity detection	13
2.8. Direct-conversion receiver	14
2.9. Frequency translation in a homodyne receiver	15
2.10. Single-conversion superheterodyne receiver	16
3.1. Photo of the completed kit.	18
3.2. First radar developped by Forstén.	19
3.3. Redesigned coffe-can radar system made by National Instruments.	20
4.1. Block diagram of the FMCW Radar Design.	22
4.2. Photo of the completed kit.	24
5.1. ADS block diagram.	25
5.2. Results of the simulation	25
5.4. Frequency vs tunning voltage	26
5.7. Gain compression at 5.5GHz.	27
5.8. Gain and return loss of the amplifier with input power set to -11dB.	28
5.9. The Wilkinson power divider. (a) An equal-split Wilkinson power divider in microstrip form. (b) Equivalent transmission line circuit.	29
5.12. This diagram demonstrates the configuration of the designed Vivaldi antenna	31
5.13. Geometry of the proposed vivaldi antennas, (a) top view of antenna, (b) bottom view of antenna	31
5.14. Reflection coefficient	32
5.15. Impedance variation with frequency	32
5.16. Radiation pattern of the antenna vivaldi at different frequencies.	33
5.17. Gain variation with frequency	33
5.19. Comparasion of the simulation with the experimental results	34
5.20. Radar board with the two antennas attached	35
5.22. Lab setup to test the FMCW Radar	35
5.23. Initial FMCW Radar Layout	36
5.24. Modified PCB layout of the initial FMCW Radar.	36

6.1. Flow diagram of the project	37
6.2. Workbench structure of the project.	38
A.1. https://www.analog.com/media/en/technical-documentation/data-sheets/hmc218b.pdf	45
A.3. https://www.analog.com/media/en/technical-documentation/data-sheets/hmc430.pdf	46
A.5. https://www.analog.com/media/en/technical-documentation/data-sheets/hmc311lp3.pdf	46
A.7. https://www.analog.com/media/en/technical-documentation/data-sheets/hmc717a.pdf	47

List of Tables

2.1. Standard Radar Frequency Letter-Band Nomenclature(IEEE Standard 521-2002)	16
5.1. Design parameters of the proposed antenna	32
6.1. Bill of materials of the FMCW radar	40

1. Introduction

Applied electromagnetism or () engineering as a field of study is not always the favourite subject of the undergraduate student. Students must first understand the fundamentals in order to achieve the necessary level of understanding to work on the more interesting applications. Understanding the fundamental background requires numerous courses over years of study and generally these courses tend to be tedious, difficult, and often discouraging to students.

Generally speaking its seen that a good understanding or good background knowledge in RF Engineering is not important and seemingly unrelated with Electrical Engineering. Far from reality, nowadays, embedded microprocessor clock frequencies have risen well above 100 MHz. Radiated waves are able to induce noise in the neighboring traces and circuit boards, which act like a small antennas. Due to these signals neighboring are susceptible to malfunction. Furthermore, plethora of nearby wireless RF devices that might interfere with operation of an electronic system. Due to that, stringent regulatory standards must be satisfied before a product may be marketed.

This only represent a one example of the whole picture of the role that electromagnetic theory plays in our society. Furthermore, unfortunately, RF laboratory equipment is expensive and normally is only accessible in research stages but not in the undergrad studies. This means that students at the undergrad level have not acquire hands on experience with basic RF devices such as LNAs, Mixers, Oscillators nor to say with RF systems such as radio transmitters or radio receivers. With that idea in mind the () is an oportunity to generate interest in applied electromagnetics and to play with.

is a detection system that is used to detect a remote object and gather important information about it. s have wide applications such as remote sensing, air traffic control (ATC), weather prediction, law enforcement in highway traffic, space applications, military and many more.

1.1. Main aim and scope of the project

The primary purpose of this project is design and implement an () system centered at 5.8 GHz which can perform range, Doppler, and synthetic aperture radar (SAR) measurements. The project is done with a modular design approach and it has the following deliverables

- RF front end board

- Tx/Rx Antennas both Vivaldi type.

1.2. Target audience

The target audience of this project encompasses educational institutions or any individual affiliated or not to any educational institution. All of the outputs of the project will have a MIT License and will be available at github.

1.3. Methodology

First the conceptual design is translated to an architectural design to verify that the radar with the choosed architecture functions as expected. To accomplish that ADS Keysight is used. Then an antenna modeling is done using via scripting in matlab language. Once is verified that the radar system, the antenna and the Wilkinson works as expected the schematic entry of the radar is done following the datasheets and the application notes of the manufacturer of the selected components. One of the most tricky parts of the system is the Wilkinson divider since its not simulated with silkscreen layer. Its recommended to isolate the modules and test it before mounting the whole system. All the PCBs are standard FR4 with 0.8mm of thickness.

1.4. Facilities

All the work is done with the equipment provided by the faculty of physics. The testing boards were done at the laboratory and the final ones were sended to JLCB Manufacturer.

1.5. Bachelor thesis outline

The following chapters of the report are organized as follows:

- **Chapter 1**, provide some brief background information concerning the project, also includes the main aim and the scope of the project, methodology intended to employ to solve the problem, where the project will be carried out and who is the target audience of this project
 - **Chapter 2**, provides a general background in radar systems. The chapter is focused on radar systems.
-

- **Chapter 3**, is devoted to a critical review of the technical and academic literature on previous work on the project.
- **Chapter 4**, Presents a brief discussion regarding the frequency regulation that applies on short range devices such as radar systems.
- **Chapter 5**, Requirements analysis is devoted to what extend the system will be and alternative solutions.
- **Chapter 6** This chapters explains the results obtained.
- **Chapter 7** Gives the timming execution diagrams such as the Gantt of the project, also includes the economic viability.
- **Chapter 8** The document finishes with a conclusion of all the work done and some future work that can be done.

2. Radar systems overview

2.1. Radar principle

The basic principle of radar consist of a transmitter that radiates electromagnetic waves of a particular waveform and a receiver that detects the echo returned from the target. The echo returned strongly depends on the particular object but in general not all the send signal is returned back, which is then amplified, down-converted and processed. The range to the target can be evaluated from the time excursion experienced by the wave. The relative velocity of the target is determined from the doppler shift of the returned signal.

In general, radars can be classified as continuous wave or commonly known as **Doppler Radar**, and pulsed **Radar**. A continuous wave radar transmits a continuous signal. In contrast, a pulsed Radar transmits a pulsed waveform, generally a train of narrow rectangular pulses modulating a sine wave carrier.

2.2. Radar Equation and System Considerations

The first equation that we are going to derive is the radar range equation. It's the most basic equation and it gives the range in terms of the characteristics of the transmitter. Consider the following simple configuration as shown in Fig. 2.1

Before we go deeper with math let's make some educated guesses on what R_{max} may be related to. It's clear that if we send out more power, R_{max} would increase. Alternatively, one could increase the gain of the antenna to increase the effective radiated power, that is, to concentrate the total radiated power towards the target direction (assuming we know where the target is). R_{max} should also be target dependent. If the target is large and reflective, then it will reflect more power and is easier to detect. Correspondingly, the R_{max} would be larger for such a target. Lastly, R_{max} should depend on how sensitive the receiver is.

Having done some qualitative analysis, let us now move on to some derivations. The radiated power density at a distance R from a radiating antenna is

$$I_t = \frac{P_t G_t}{4\pi R^2},$$

where P_t is the transmitted power and G_t is the gain of the transmitting antenna.

Now the amount of power reflected from a target at a distance R is not only dependent on

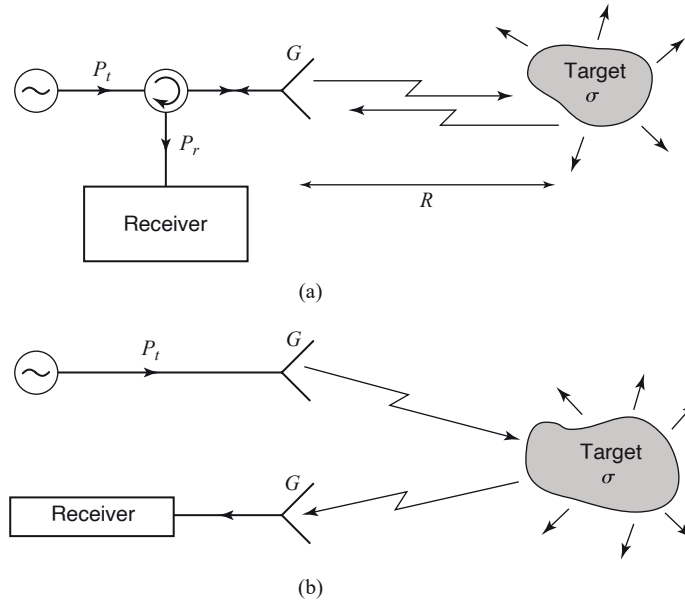


Figure 2.1: Basic radar system.

I_t , but also on the target size, geometry, and material reflectivity. All of this can be captured into a single quantity, called the radar cross section (RCS) which has a dimension of area. Basically, a target with RCS of σ looks like a perfect spherical reflector of cross-sectional area σ^1 and the reflected power is

$$P_\sigma = \frac{P_t G_t \sigma}{4\pi R^2}.$$

Another assumption in the calculation and measurement of RCS is that the reflected power is assumed to be isotropic towards all directions. With this assumption in mind, the received power intensity at the location of the radar is

$$I_r = \frac{P_t G_t \sigma}{4\pi R^2} \frac{1}{4\pi R^2}.$$

The received power at the radar receiver is then

$$P_r = \frac{P_t G_t \sigma}{4\pi R^2} \frac{A_{eff}}{4\pi R^2},$$

where A_{eff} is the effective aperture of the antenna and is related to the gain of the antenna by

$$G_r = \frac{4\pi A_{eff}}{\lambda^2}.$$

¹The radar cross section of a target is the effective (or fictional) area defined as the ratio of the backscattered power to the incident power density. The larger the RCS, the higher the power backscattered to the radar. The RCS depends on the size, shape, materials, the frequency and polarization of the incident wave, and the incident and reflected angles relative to the target.

Therefore,

$$P_r = \frac{P_t G_t \sigma}{(4\pi R^2)^2} \frac{G_r \lambda^2}{4\pi} = \frac{P_t G_t G_r \lambda^2 \sigma}{(4\pi)^3 R^4}.$$

Solving for the range R we obtain the radar range equation

$$R = \sqrt[4]{\frac{P_t G_t G_r \lambda^2 \sigma}{P_r (4\pi)^3}}. \quad (2.1)$$

The radar range equation gives a reasonable estimate of the maximum range of a radar at a given transmitter power and receiver sensitivity. Note that we considered that there are no missalignment, no polarization mismatch, no loss in the atmosphere, and no impedance mismatch at the antenna feed. Also the target is assumed to be located in the far-field region of the antenna.

Let account for the fact that there is minimum receiver signal below of which the the radar will not be able to detect the target. Let the minimum allowable signal power $P_r = S_{i,\min}$ then we have

$$R = R_{\max} = \left(\frac{P_t G_t G_r \sigma \lambda^2}{(4\pi)^3 S_{i,\min}} \right)^{1/4} \quad (2.2)$$

where

- P_t = transmitted power (W)
- G = antenna gain (linear ration) unitless
- σ = radar cross sectionm²
- λ = free-space wavelenght(m)
- $S_{i,\min}$ = minimum receiving signal (W)
- R_{\max} = maximum range (m)

This is the radar range equation. The maximum radar range (R_{\max}) is the distance beyond which the required signal is too small for the required system operation. This is the radar equation. Note that the received power varies as $1/R^4$, which implies that a high-power transmitter and a sensitive low-noise receiver are needed to detect targets at long ranges. Let rewrite the eq 2.2 in terms of the noise factor.

The noise factor of a receiver is defined as

$$F = \frac{S_i/N_i}{S_o/N_o} \quad (2.3)$$

where S_i and N_i are input signal and noise levels, respectively, and S_o and N_o are output signal and noise levels, respectively at the receiver. Since $N_i = kTB$ we have

$$S_i = kTBF \left(\frac{S_o}{N_o} \right) \quad (2.4)$$

where k is the Boltzmann factor, T is the absolute temperature, and B is the bandwidth. When $S_i = S_{i,\min}$, then $S_o/N_o = (S_o/N_o)_{\min}$. The minimum receiving signal is then given by

$$S_{i,\min} = kTBF \left(\frac{S_o}{N_o} \right)_{\min} \quad (2.5)$$

Substituting this into Eq. 2.2 gives

$$R_{\max} = \left[\frac{P_t G_r G_t \sigma \lambda_0^2}{(4\pi)^3 k T B F \left(\frac{S_o}{N_o} \right)_{\min}} \right]^{\frac{1}{4}} \quad (2.6)$$

where $1.38 \times 10^{-23} \text{ J/K}$, T is temperature in kelvin, B is bandwidth in hertz, F is the noise figure in ratio, $(S_o/N_o)_{\min}$ is minimum output signal-to-noise ratio in ratio and is determined by the system requirements.

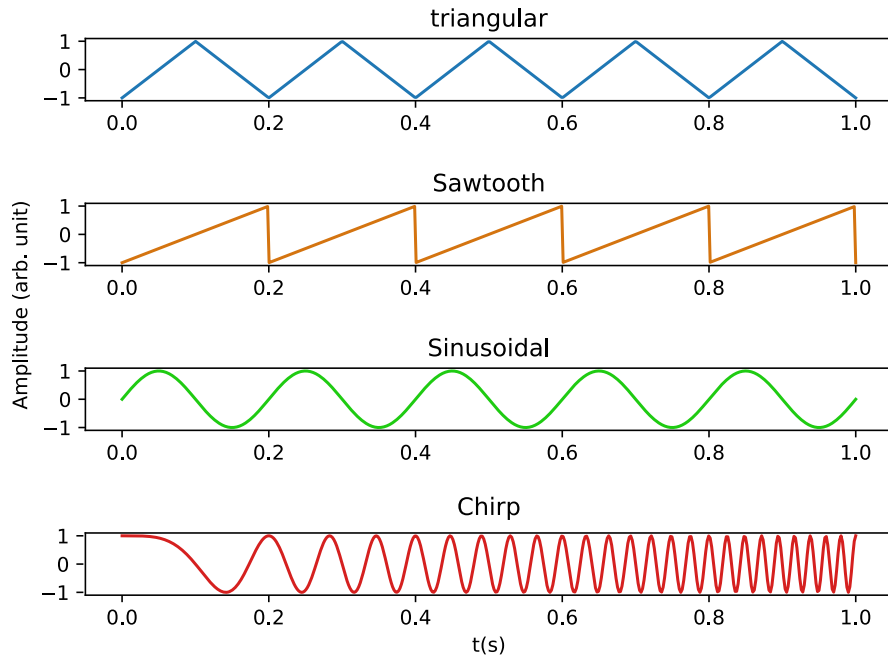
2.3. Modulation Patterns

Several types of frequency modulation can be used. In this section, some of them are explained along with the specific features or applications. These types are:

- Linear frequency modulation: like sawtooth or triangular. This is the most frequently used modulation. Sawtooth modulation cannot measure Doppler frequency; it appears as an added noise in the received signal. On the other hand, triangular frequency modulation can measure both distance and velocity. However, if there are multiple objects, the Doppler frequencies cannot be uniquely associated with a target.
- Sinusoidal: This modulation is easy to generate and produces a narrow spectrum. Some applications of this modulation are low-range altimeters, level measuring radar and

sensors of mobile targets.

Figure 2.2: Typical modulation patterns.



2.4. Doppler Effect and () Radar

A () radar or doppler radar is the most simple type of radar. It can be used to detect a moving target and determine the velocity of the target. If there are relative motion between the radar and the target then we will have some sort of frequency shift due to Doppler effect, the angular excursion or phase ϕ made by the electromagnetic wave during its transit to and from the target can be used to extract the velocity from the target. If R is the distance of the target from the RADAR antenna, then the total number of wavelenghts contained in the two-way path is $2R/\lambda$, where λ is the wavelenght. The corresponding phase shift is as follows:

$$\phi = 2\pi \times 2R/\lambda = 4\pi R/\lambda \text{ rad} \quad (2.7)$$

If the target is moving, then R and hence ϕ are continuously changing with time. The variation of ϕ with time gives the angular frequency:

$$\omega_d = 2\pi f_d = \frac{d\phi}{dt} = \frac{d}{dt}(4\pi R/\lambda) = \frac{4\pi}{\lambda} \frac{4\pi}{\lambda} \frac{dR}{dt} = \frac{4\pi}{\lambda} v_r \quad (2.8)$$

where f_d is the Doppler frequency and v_r , the relative velocity of the target. From Eq.2.8, we can write that $f_d = v_r/\lambda$. If the target is moving at an angle θ , then

$$v_r = v \cos \theta \quad (2.9)$$

Substituting Eq. (2.9) into Eq. (2.8), we get $f_d = 2v \cos(\theta)/\lambda$. From this result we see that

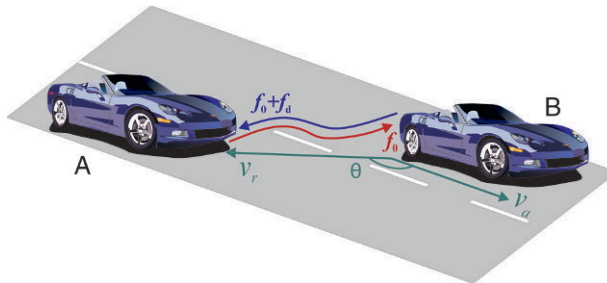
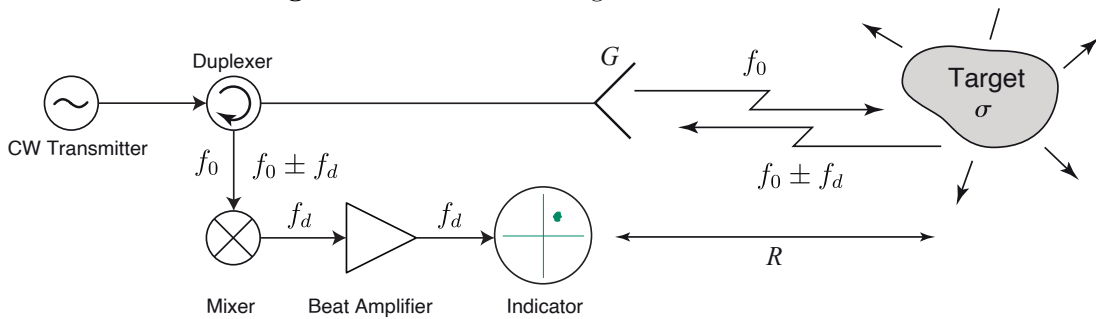


Figure 2.3: Target moving at an angle θ .

Doppler shift is maximum when $\theta = 0^\circ$ and is equal to zero $\theta = 90^\circ$. In fact, this is only true if the speed of the target is $v_r \ll c$. In special relativity the observer will see a change in frequency or wavelength, even though the distance between observer and source at that instant is not changing. This effect is due relativistic time dilation rather than of a true Doppler effect, this is known as “transverse Doppler effect”, ² [1],[2]. The magnitude of Doppler shift is same regardless of whether the target is moving towards the RADAR (positive shift) or away from it (negative Doppler shift). The received signal frequency will be higher than the transmitted signal frequency if the target is moving toward the RADAR and lower than the transmitted signal frequency in the opposite case. The basic block diagram of a Radar is

Figure 2.4: Basic block diagram of CW RADAR.



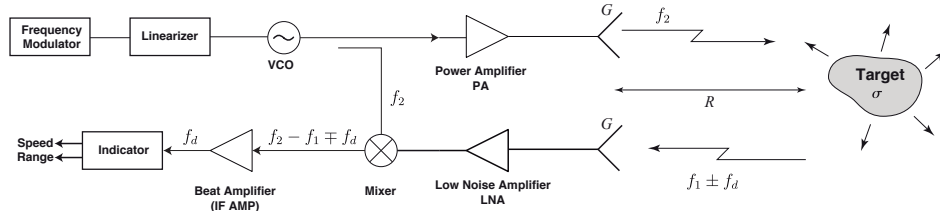
²The advent of particle accelerator technology has made possible the production of particle beams of considerably higher energy than was available to Ives and Stilwell. This has enabled the design of tests of the transverse Doppler effect directly along the lines of how Einstein originally envisioned them, i.e. by directly viewing a particle beam at a 90° angle. For example, Hasselkamp et al. (1979) observed the $H\alpha$ line emitted by hydrogen atoms moving at speeds ranging from 2.53×10^8 cm/s to 9.28×10^8 cm/s, finding the coefficient of the second order term in the relativistic approximation to be 0.52 ± 0.03 , in excellent agreement with the theoretical value of $1/2$

show in Fig. 2.4. The transmitter generates a signal of frequency f_0 , whereas due to the Doppler shift the received signal will be of frequency $(f_0 \pm f_d)$. The received signal is mixed with the transmitted one in a mixer to obtain the Doppler frequency f_d . Note that the sign of the Doppler shift is lost in this process. The resultant signal is then amplified and sent to the indicating device or to some sort of processing device. It should be noted that clutters (stationary objects) do not provide any Doppler shift and hence are not detected by the Doppler radar. This is an inherent advantage of a Radar. In addition this kind of radars uses a low power transmitting circuitry and in general it has a small size compared to the pulsed radars. When developing a radar system it must be considered the use of a separated receiver and transmitter antennas because in general gives a better performance due to the isolation between the receiver and transmitter circuitry.

2.5. () Radar

We have seen in the previous section that the CW radar has the disadvantage that it cannot determine target range because it lacks the timing mark necessary to allow the system to time accurately the transmit and receive cycle. In a frequency-modulated Radar or (), frequency

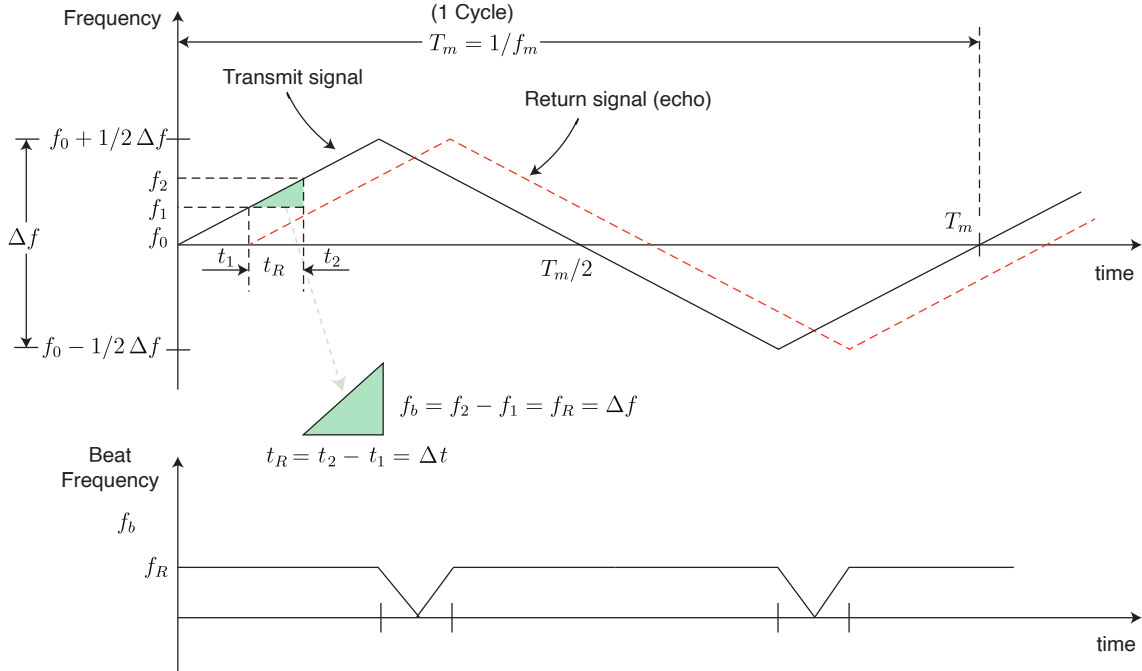
Figure 2.5: Basic block diagram of FMCW RADAR.



of the transmitted signal changes with time in a known manner. Due to this, unlike a Doppler Radar, the frequency of the echo signal and the transmitted signal, at the instant the echo is received, is not the same, more precisely, this change in frequency is the timing mark we need to extract the range. Thus, the transmitting time is determined from the difference in frequency between the transmitting signal and the returned signal. Figure 2.5 shows a block diagram of a FMCW radar. Here, a voltage-controlled oscillator is used to generate an FM signal. A two antenna system is shown this gives a better isolation improvement between the transmitter and the receiver. The returned signal is $f_1 \pm f_d$. The plus sign stands for the target moving toward the radar and the minus sign for the target moving away from the radar. Let us consider the following two cases: The target is stationary, and the target is moving.

2.5.1. Stationary-Target Case

If the distance of the target from the Radar is R , then the transit time of the signal to reach the receiver is $t_2 = t_1 + t_R = t_1 + 2R/c$. If the echo signal is heterodyned with a part of the

Figure 2.6: Basic block diagram of FMCW RADAR.

transmitter signal, then due to the frequency difference between the signals, a beat note f_b is produced. Since the target is stationary, the beat note f_b is due to the range only. Hence

$$f_R = f_b = f_2 - f_1 \quad (2.10)$$

From Fig. 2.6 we see that the variation rate of the frequency is

$$\dot{f} = \frac{\Delta f}{\Delta t} \quad (2.11)$$

We can also calculate the frequency variation observing in Fig. 2.6 that the frequency experiences an excursion of $2\Delta f$ in one cycle, which is equal to $T_m = 1/f_m$. Hence,

$$\dot{f} = \frac{2\Delta f}{T_m} = 2f_m\Delta f \quad (2.12)$$

Equating Eqs. (2.11) and (2.12) we have

$$f_b = f_R = t_R \dot{f} = 2f_m t_R \Delta f \quad (2.13)$$

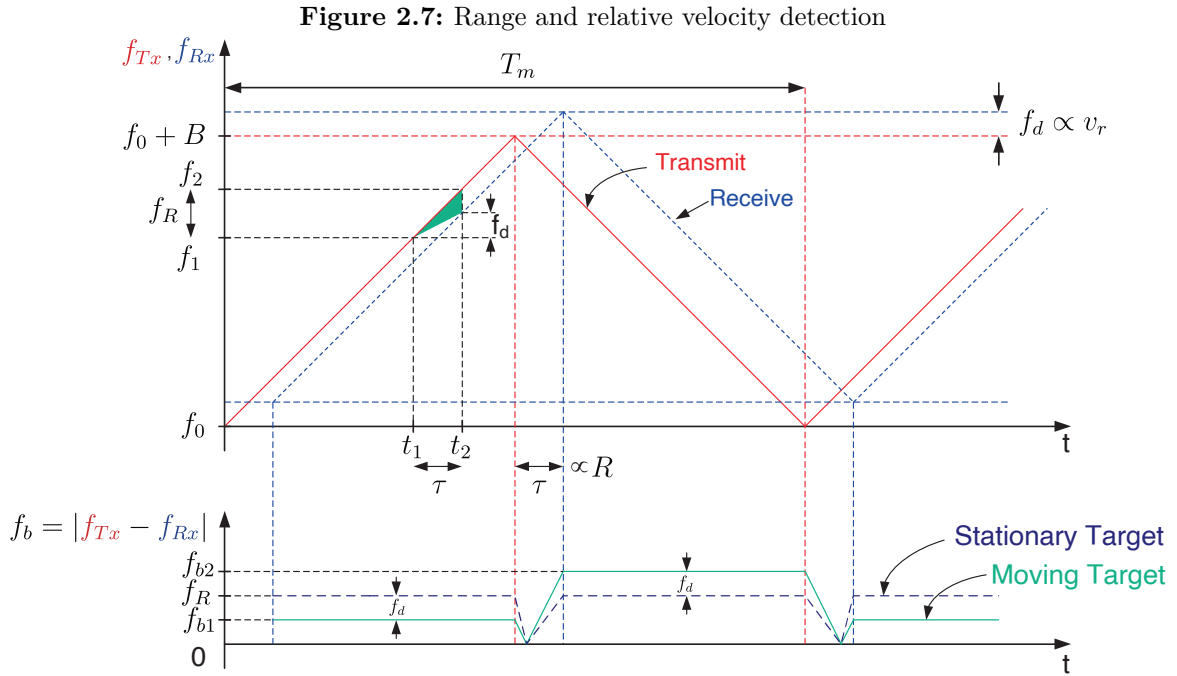
Substituting $t_R = 2R/c$ into (2.13), we have

$$R = \frac{c f_R}{4 f_m \Delta f} \quad (2.14)$$

Notice that in the derivation we supposed that the frequency is varying with time in a linear manner. In any practical Radar, the frequency cannot be increased or decreased continuously, and hence periodicity in the modulation is required. The nature of modulation may be saw-tooth, triangular, sinusoidal, or some other function as shown in Fig. 2.2. The variation of frequency is known since it is set up by the system design also the modulation rate (f_m) and modulation range (Δf) are known.

2.5.2. Moving-Target Case

In the previous discussion, we assumed that the target is stationary. If this is not true, then a Doppler shift will be superimposed on the FM beat note. In the frequency-time plot, this Doppler frequency shift will shift the absolute values of the received frequencies up or down, as shown in 2.7. Thus, the downconverted frequencies are,



$$f_b = |\mathbf{f}_{Tx} - \mathbf{f}_{Rx}| \quad (2.15)$$

$$f_{b1} = f_R - f_d \quad (2.16)$$

for the raising and for the falling slope of the transmit signal, respectively. Notice that the range information is in f_R and the velocity information is in f_d . Once the beat frequency levels f_{b1} and f_{b2} have been measured in the baseband, the range and the relative speed can be calculated by

$$R = \frac{c(f_{b1} + f_{b2})T_m}{8B} \quad (2.17)$$

$$v_r = \frac{c(f_{b1} - f_{b2})T_m}{4f_0} \quad (2.18)$$

where f_0 is the frequency of the transmitted signal. In the presence of multiple targets, at different ranges, the radar mixer output will contain multiple frequency components. By measuring each frequency component, the range of each target can be determined.

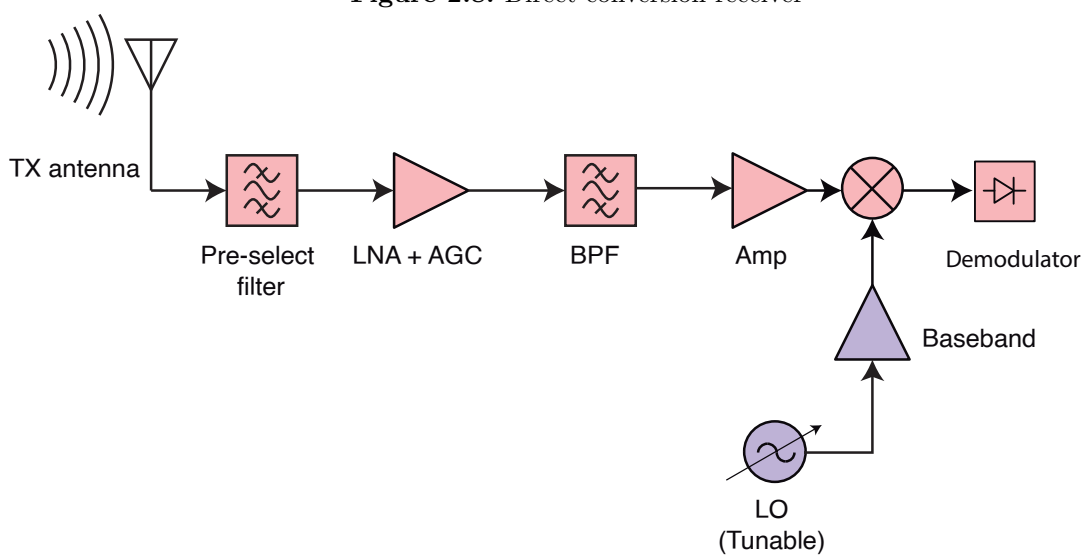
2.6. Receiver Architectures

A radar receiver performs the task to detect the scattered signal from the target, amplify without adding extra noise and down-convert the signal. Therefore, the requirements for the receiver performance are usually very demanding. It's desirable for a radar that it has a high dynamic range, good isolation between the RF and LO signals to avoid to suffer leakage between them, and a low noise performance in reception. In general, receiver architectures are classified by their down-conversion topology.

2.6.1. Homodyne

The homodyne or also known as direct down-conversion receiver has the most simple architecture and translates the signal directly to zero-IF. Note that the frequency of the local oscillator (LO) is equal to the carrier frequency of the received RF signal.

Figure 2.8: Direct-conversion receiver



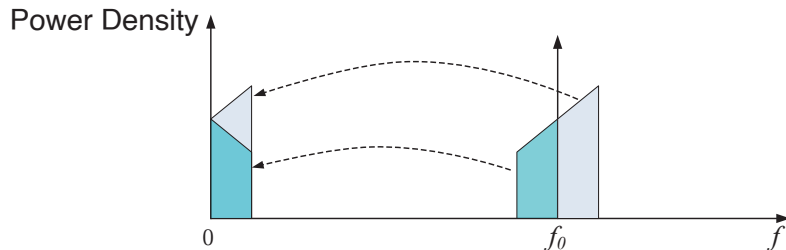
The signal scattered from the target is applied to the RF input of the mixer and mixed with the local oscillator signal applied at the LO input. If the local oscillator signal has the same center frequency as the RF input, then we will get a DC signal at the output or zero-IF. In figure 4.1 we see the block diagram of the radar architecture. The advantages of homodyne receivers are listed as follows.

1. Minimum components
2. Low cost.
3. Multiple stages are unnecessary
4. No image frequency issues

Also, this architecture suffers from the disadvantages listed below

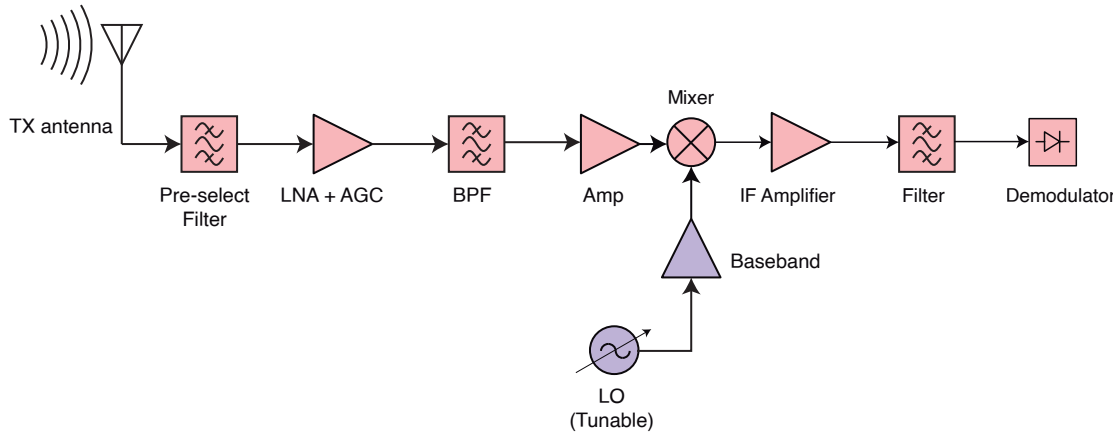
1. LO leakage into front-end RF system that can drive the system to have a large DC offset values. This is due to the low isolation between the LO and the LNA input, the LO signal leaks to the LNA input. This in turns re-enters the receiver along with the RF signal and mixes with the LO.
2. High flicker noise

Figure 2.9: Frequency translation in a homodyne receiver



2.6.2. Single-Conversion Superheterodyne Receiver

Another possible choice for the receiver architecture could be the Single-Conversion Superheterodyne Receiver. Here the RF signal is filtered through a wideband bandpass filter to a mixer. Also feeding the mixer there is a signal that in general would be tunable and only differs from the signal by an amount equal to

Figure 2.10: Single-conversion superheterodyne receiver

2.7. Spectrum regulation

The development of advanced wireless system has to take account of spectrum regulation. The radar works in the C-band spectrum typically used by meteorological radars. As is stated in The power delivered by a transmitter to the antenna of a station in the fixed or mobile services shall not exceed +13 dBW in frequency bands between 1 GHz and 10 GHz, or +10 dBW in frequency bands above 10 GHz, except as cited in No. 21.5A. (WRC-2000).

Table 2.1: Standard Radar Frequency Letter-Band Nomenclature(IEEE Standard 521-2002)

Band Designator	Frequency (GHz)	Wavelength in Free Space (centimeters)
HF	0.003 to 0.030	10000 to 1000
VHF	0.030 to 0.300	1000 to 100
UHF	0.300 to 1	100 to 30.0
L band	1 to 2	30.0 to 15.0
S band	2 to 4	15 to 7.5
C band	4 to 8	7.5 to 3.8
X band	8 to 12	3.8 to 2.5
Ku band	12 to 18	2.5 to 1.7
K band	18 to 27	1.7 to 1.1
Ka band	27 to 40	1.1 to 0.75
V band	40 to 75	0.75 to 0.40
W band	75 to 110	0.40 to 0.27
mm	110 to 300	0.27 to 0.10

When operating the radar we should take care of the frequency operating of the device since the frequencies between 5 and 6 GHz are used by different services.[3]

3. Background and related work

3.1. Historical background

The basis of (RAdio Detection And Ranging) theory dates back to the beginning of the 20th century. As it was originally conceived, radio waves were used to detect the presence of a target and to determine its distance or range. It was clear the havoc that Hitler's Luftwaffe had inflicted on cities and the civilian population during the Spanish Civil War. It suddenly became clear that waves of enemy bombers could fly over their cities levelling them in a rain of bombs with absolutely nothing to warn of their approach.

On February 12, 1935, in a secret report entitled "The detection of aircraft by radio methods" and with the experimental demonstration carried out on February 26, 1935, led Robert to be the inventor of the first radar system. This radar broke the back of Hitler's air force by detecting German bombers even before they approached their targets, allowing the British Royal Air Force to concentrate its limited combat resources on the most powerful threats to the population. civilian and the machinery of war.

Much has changed since that era but the radar techniques has since been adopted for civil applications such as obstacle detection on-board air planes and ships, traffic control in airports, long distance measurements, and remote sensing. Recent advances in silicon technologies and electronic design methods, make possible the realisation of highly integrated radars with low cost, compact size, and low power consumption. This enables the widespread adoption of radar for new civil and defence applications such as: automotive () for car parking, side-crash warning, collision warning,; SRR for contact less heart and pulmonary monitoring in e-health applications, mm-wave body scanner for security and many more.

Since there are many radar technologies in this bachelor thesis we focus mainly in () radar systems. radars are often called "radars of the future". This is because today, almost every radar -X band and higher - uses this technology, and are widespread used in all kinds of applications.

3.2. Previous work

In 2012, IEEE Spectrum published an article titled, Coffee-can Radar: How to Build a Synthetic Aperture Imaging System with Tin Cans and AA Batteries. This article described how to build a synthetic aperture radar using a laptop coffee-can radar system that was derived

from the OpenCourseWare (OCW) online free course materials provided through MIT. This course was done in January 2011 during Independent Activities Period (IAP) MIT Lincoln Laboratory sponsored a radar short course at MIT campus [4]. The objective of this course was to generate student interest in applied electromagnetics, antennas, radio frequency (RF) electronics, analog circuits, and signal processing by building a short-range radar sensor - also known as coffee can radar - and using it in a series of field tests. To make this radar system accessible to students, a low-cost radar kit was developed by the authors with a total cost of \$360 in materials per kit. The radar kit was an S-band FMCW radar centered at 2.4 GHz with less than 20 mW of transmit power. Moreover to reduce the cost the antennas were made from coffee cans in an openended circular waveguide configuration. The whole system was mounted on a block of wood providing a clear outline of the radar's design. The analog signal chain was implemented on a solderless breadboard for quick fabrication and easy modification. Finally, to make the kit portable it runned on eight AA batteries.

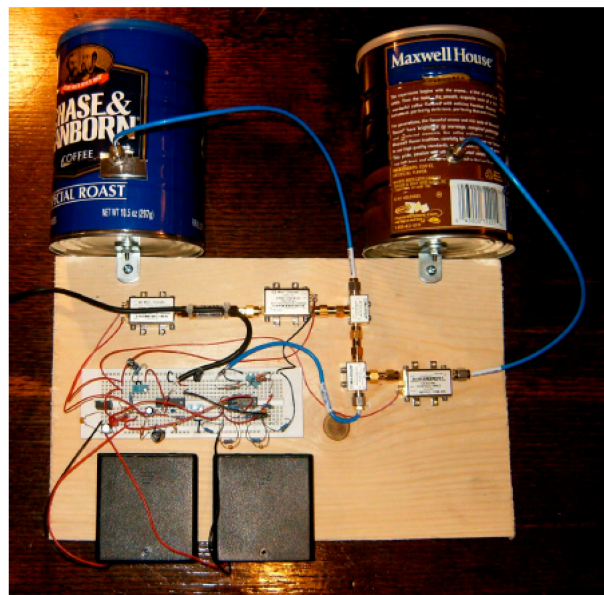


Figure 3.1: Photo of the completed kit.

Since then many others tried to reproduce and enhance the radar system made at IAP. A finish engineer Henrik Forstén a researcher at VTT made a very simple frequency-modulated continuous-wave (FMCW) radar that was able to detect distance of a human sized object to 100 m. The radar made by Forstén was fit entirely on a PCB using surface mount components in contrast with Charvat radar that followed a modular approach with discrete components. The major advantage of using surface mount components is the required space and One disadvantage in this application is the equal division of the power. We would like most of the power to go to the transmission antenna and only a little bit to the mixer. With equal division there needs to be an attenuator before the mixer to make decrease the input power. This is a wasted power that should be used in transmission. More complicated power splitter would add too much board area to be worth it, even the simple Wilkinson splitter uses large amount

of the board compared to how many components could be fit into the space it uses. Its better to use a Coupler divider than the wilkinson since the coupler can give to the transmitting path more power than to the receiver path.

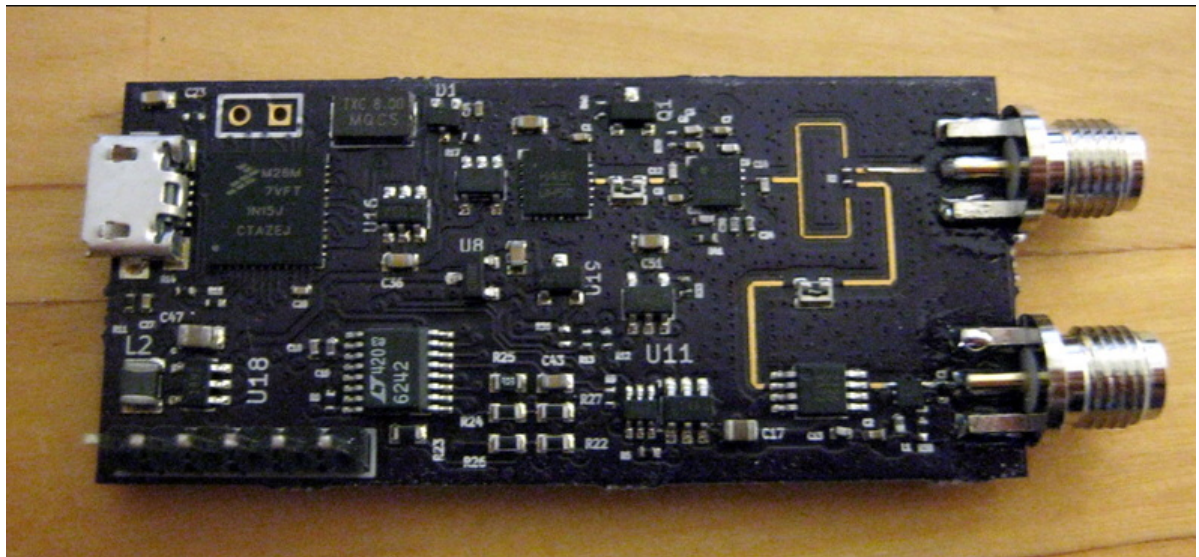


Figure 3.2: First radar developed by Forstén.

At UC Davis, Prof. ‘Leo’ Liu’s made full-semester senior design course based on the MIT Coffee Can radar short course. Looking at previous works made by the students its seen that following a modular approach its better for debugging and troubleshooting purposes [5] because is very important that we provide many test points on the first design because we will need to test that each part is working correctly. So, the first design is better to follow a modular approach, splitting the design into multiple segments and create a smaller PCB for each.

Also, it's seen that to improve the RF system, the noise should be diminished. In order to do so, following the discussion of the noise source, a 4 layer board with a better dielectric could be used, to better contain the RF signals. This would bring the ground plane closer to the RF traces, increase the capacitance, decrease the size of the RF traces, and increase the isolation between the traces. Another major drawback for the system is the noise. As the signal goes further and further out, the IF signal quickly diminishes into the noise floor, limiting how far out we can see. The signals being transmitted are too high frequency and too high power for the FR-4 material, and are leaking out into the rest of the board.

Finally, another project that its worth to take a look is the radar project developed by National Instruments (NI). NI, redesigned the original coffee-can radar system. The re-caffeinated coffee-can radar system design was done with NI AWR high-frequency software in order to get good performance smaller footprint and a less costly BOM. The VCO, PA, and LNA were all produced directly from the layout shown on the datasheets. The 1dB attenuator, the low pass filter, and the board coupler were all designed in Microwave Office circuit design software,



Figure 3.3: Redesigned coffe-can radar system made by National Instruments.

and AXIEM was used to design the coupler. The final board has a dimensions of $3'' \times 3''$ inches, and the final BOM ascends no more than \$60, this was much less expensive than the original design with BOM components consting \$250. Unfortunately the performance of this radar is not provided in this application note.

4. Requirements analysis

This chapter is devoted to make an analysis of the requirements of the radar system. First in section 4.1 a radar architecture is selected. Then in 4.2 is discussed the purpose of the needed components for the Radar. The chapter finishes with a discussion of the selected components and possible alternative configurations and architecture selection for the radar.

4.1. Architecture selection

A homodyne receiver is selected due to its small size and low parts count. In the Fig 4.1 we have a basic diagram of the radar system. In green we have the transmitter path and in red we have the receiver path.

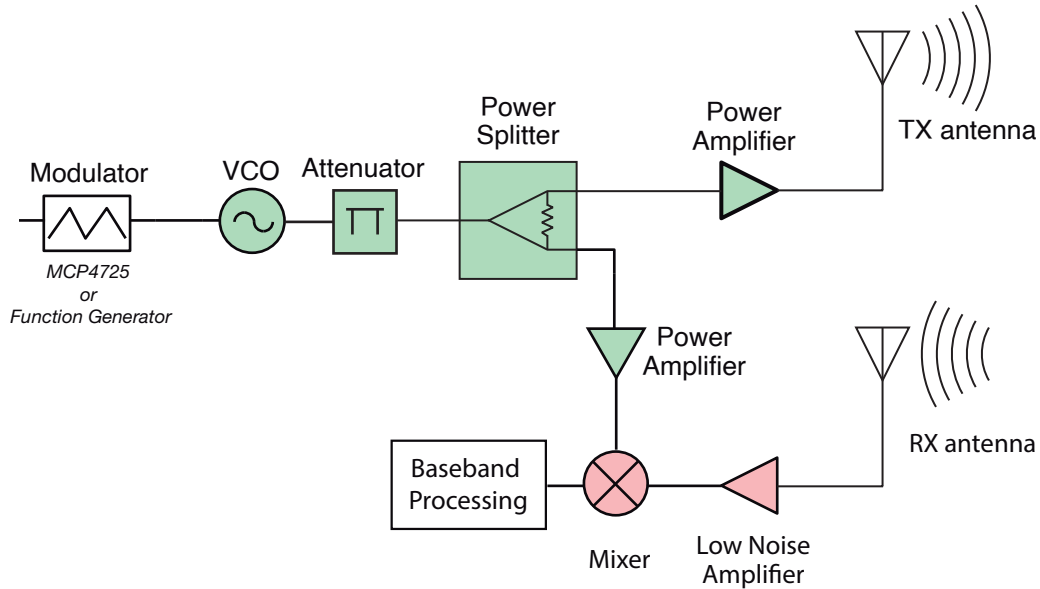
4.2. Description of the modules

4.2.1. Transmission elements

A radar transmitter should generate a frequency signal of interest, amplify the signal to a power level sufficient to reach certain desired level and radiate that signal into the environment through an antenna. The signal will either see an object and scatter, or it will eventually propagate far enough that it is naturally absorbed into the atmosphere or proceed further to travel into space. Below are described the elements found in the transmission path, vide Fig. 4.1 TX path.

VCO	Outputs a frequency in linear proportion to its input control voltage (Vtune). FM is achieved by changing VCO Vtune input over time. There are different modulating patterns that can be applied to VTUNE input depending on the application that we are interested. In this case we are going to modulate Vtune with Triangular modulation pattern. This kind of modulation allows easily separation of the difference frequency Δf of the Doppler frequency f_d . The output of VCO is then a sinusoidal waveform that is changing frequency over time. The selected VCO is the HMC430LP4 from the Analog Devices. The power output is 2dBm typical from a 3V supply voltage.
------------	---

Figure 4.1: Block diagram of the FMCW Radar Design.



Attenuator

Attenuators are two-port components that add loss (or remove gain) wherever they are placed. In Fig 4.1 we see an attenuator that is placed between the VCO and the power splitter. The attenuator has an attenuation of 3dB and his purpose is to lower the output power of the VCO to ensure that the power amplifiers will not saturate the amplifier if its required.

Wilkinson Divider

Power splitters (or dividers) enable signal to be split into two or more separate paths.

Power Amplifier

Amplifier optimized for high output power. The selected component is the HMC311LP3E from Analog devices. The HMC311LP3(E) offers 14.5 dB of gain and an output IP3 of +32 dBm while requiring only 56 mA from a +5V supply the maximum input power is about 10dBm.

4.2.2. Receiver elements

In the receiver path we have the RX antenna which captures the scattered signal from the target. That signal is then amplified by a Low Noise Amplifier (LNA).

Mixer

The mixer has the task to produce the beat-frequency (intermediate-frequency IF). This is done by mixing the LO signal with the received signal in the RX antenna. The mixer is the HMC218B from analog devices. This mixer performs well when used as a down-converter from 3.5 to 8 GHz and as an up-converter from 4.5 to 8 GHz. The

low conversion loss, high isolation and wide IF bandwidth make this mixer ideal for a variety of Rx and Tx frequency plans.

Low Noise Amplifier

The Low Noise Amplifier (LNA) is an amplifier specially designed to add the minimal amount of noise in the signal received. The selected LNA is the HMC717A from Analog devices. The amplifier has been optimized to provide 1.1 dB noise figure, 14.5 dB gain and +29.5 dBm output IP3 from a single supply of +5V. Input and output return losses are excellent and the LNA requires minimal external matching and bias decoupling components. The HMC717ALP3E can be biased with +3V to +5V and features an externally adjustable supply current which allows the designer to tailor the linearity performance of the LNA for each application.

4.3. PCB Materials

Due to the constraints of project the PCB board is made with a 0.8mm thickness with an FR4 base material with two layers. FR4 base material is not good for RF boards since the impedance is not controlled. Radar applications between 2.4GHz and 6GHz could be done with FR4 since parasitic losses aren't yet too high to demand using exotic substrates.

4.3.1. Wilkinson

The main task of the Wilkinson splitter is to split an input signal into two equal phase output signals. The Wilkinson is not the better option because we are interested in put more power in the transmitter path than in equally split the power. Due to the simplicity of the Wilkinson and the constraints of the time other better options such as a Coupler splitter was discarded.

4.3.2. Antenna selection

Picking the correct antenna type [6] is the first step towards a successful project. The bandwidth of the antenna will determine the biasing needed for the VCO. Having a wider bandwidth is desirable because that will improve the resolution of the radar system. Note that $R = c/2BW$. It is important to design for acceptable resolution because that will determine the radar system's ability to distinguish between two or more targets in the same vicinity at different ranges.

Usually radars use very directional horn antennas. Directionality of the beam is important so that only signal from the target is picked up instead of the surroundings. Besides the directionality radar antenna should have low sidebands so that antenna to antenna coupling is low and it doesn't pick up reflected signals from behind and sides of the radar. Also the

antennas should not reflect the power back but instead do their job and radiate it.

Maybe a pyramidal horn antenna would be a good choice it can fulfill all the specifications but it has high cost. Another option was Patch antenna but it was discarded due to it has a low fractional bandwidth.

Finally, we decided to made a Vivaldi antenna. Vivaldi antennas are useful for any frequency, as all antennas are scalable in size for use at any frequency. Printed circuit technology makes this type antenna cost effective at microwave frequencies exceeding 1 GHz.[7]

This inexpensive Vivaldi antenna is etched upon a printed circuit board and fed with a soldered-on coaxial cable and SMA connector. Advantages of Vivaldi antennas are their broadband characteristics (suitable for ultra-wideband signals), their easy manufacturing process using common methods for PCB production, and their easy impedance matching to the feeding line using microstrip line modeling methods.

5. Detailed design of the Radar

5.1. Radar System Analysis

In Fig 5.1 we have the block diagram simulation that was performed with ADS Keysight and in Fig 5.3a, 5.3b the carrier and baseband spectrum respectively.

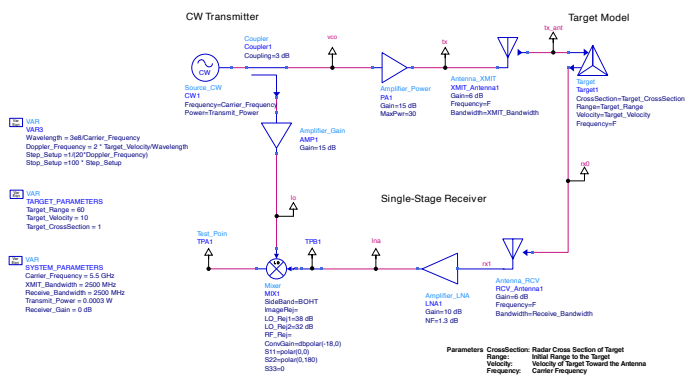
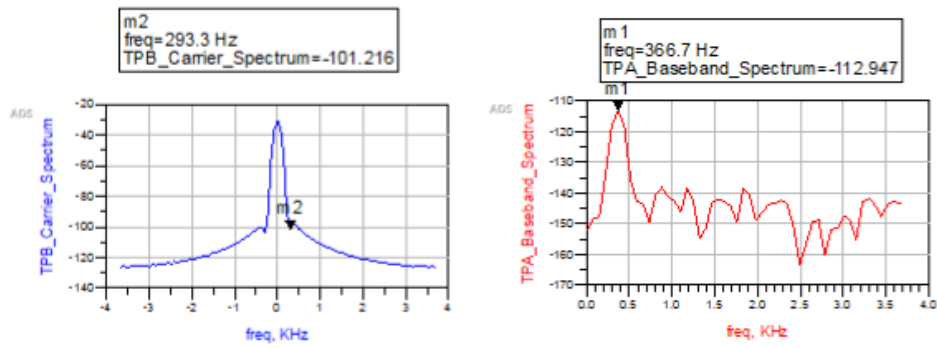


Figure 5.1: ADS block diagram.

Figure 5.2: Results of the simulation



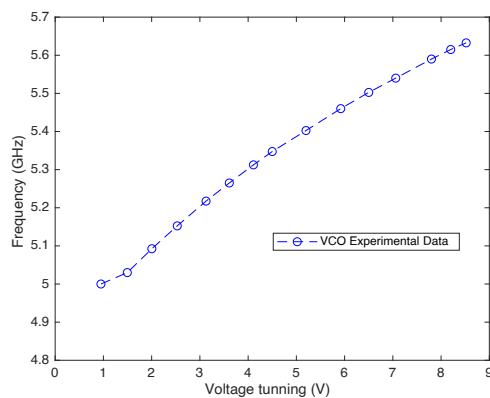
(a) Carrier Spectrum of the simulated system (b) Baseband spectrum of the simulated system

We see that the system works as expected since the transmitted signal is positively shifted.

5.2. VCO

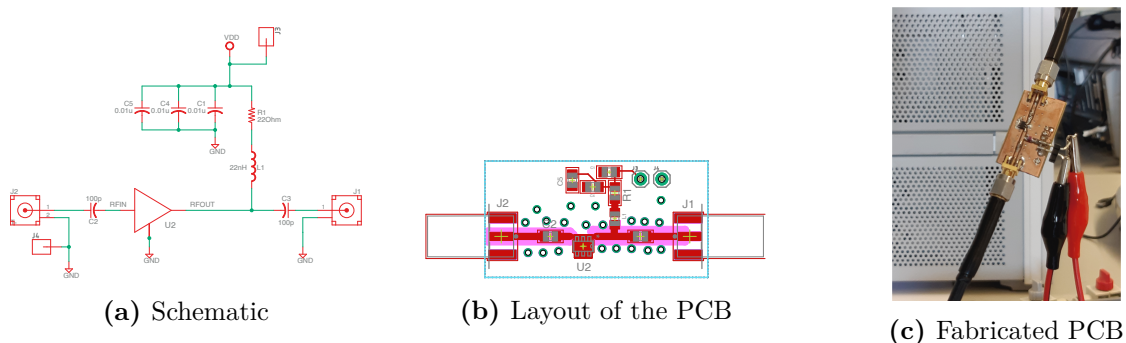
The RF signal is generated by the voltage controlled oscillator (VCO), which tuning voltage is generated by a signal generator. During the test it was found that the output power of the VCO was 2dBm-4dBm lower than the datasheet values. This could be for different reasons. The most critical one is the substrate of the PCB that we used was FR4 which has higher losses than the Rogers 4350 substrate used by the manufacturer. We can see in Fig 5.4 that the experimental is coherent with the datasheet data A.3

Figure 5.4: Frequency vs tuning voltage

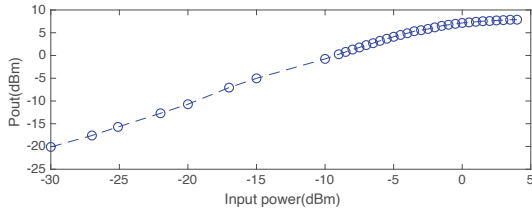


5.3. Amplifier

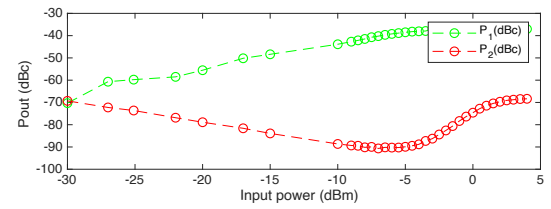
In the following picture we have the schematic, the PCB layout and the fabricated board of a dedicated test applied to the amplifier. To verify that the amplifier was function properly to test were applied. The first one to extract to power compression and the second one to extract S parameters.



The power transfer curves for an amplifier with a gain of 14.5 dB. We see that the blue curve in Fig 5.6a can deliver the gain only up to a 0dB approximately of power level before it hits saturation. Gain compression is the difference between the green curve and the red curve. An important gain compression parameter is the OP1dB which is the power input that results in a 1 dB compression. We can approximately see the OP1dB is approximately 1.5 dB because at that input power level, the red curve is at 8.5 dB and the red curve is at approximately 7.5 dB as we see in 5.7. This value is much lower than the value that we see in the page 1 of the Datasheet A.5. First of all, we should know how the manufacturer has done the tests but it is quite possible that the substrate used to make the pcb cause that discrepancy with the results found.



(a) Power compression of the input power at 5.5GHz



(b) Power compression of the 2nd and 3rd harmonic at 5.5GHz

It is observed, see Fig 5.8, that the gain of the amplifier (S_{12}) of 15 dB and return loss (S_{11} and S_{22}) of < -10 dB at the frequency of interest. This agree very well from the results that the manufacturer gives in the page 2 of the datasheet A.5.

Figure 5.7: Gain compression at 5.5GHz.

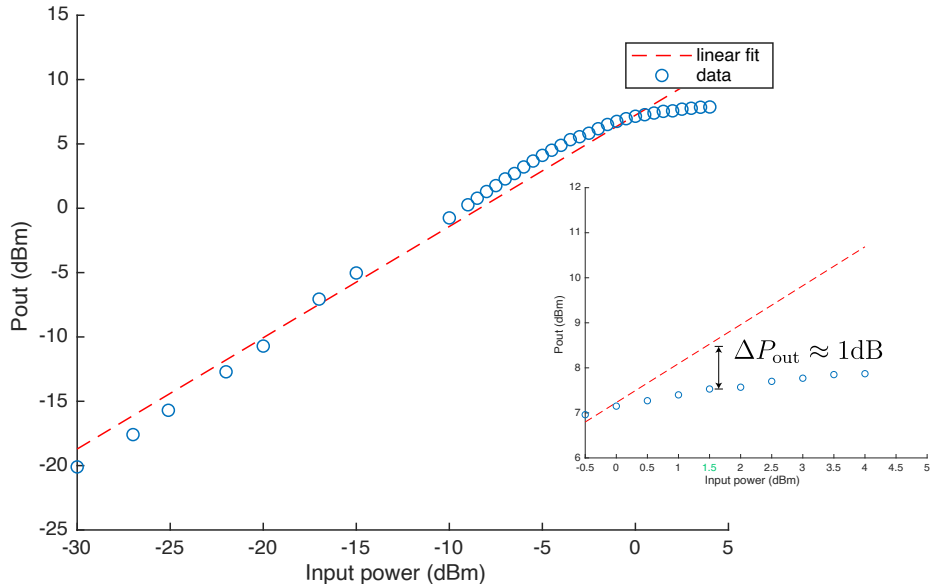
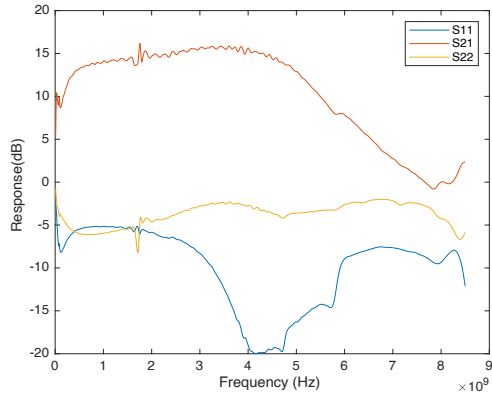


Figure 5.8: Gain and return loss of the amplifier with input power set to -11dB.



5.4. Wilkinson

5.4.1. Introduction

The Wilkinson¹ power divider splits the input power in to two equal phase output signal signals², As it is seen in Fig 5.9 relies on quarter-wave transformers to match the split ports to the common port. Let's briefly see how the Wilkinson works. When a signal enters port 1, it splits into equal-amplitude, equal-phase output signals at ports 2 and 3. Since each end of the isolation resistor between ports 2 and 3 is at the same potential, no current flows though it and therefore the resistor is decoupled from the input.

The two output port terminations will add in parallel at the input, so they must be transformed to $2Z_0$ each at the input port to combine to Z_0 . The quarter-wave transformers in each leg accomplish this; without the quarter-wave transformers, the combined impedance of the two outputs at port 1 would be $Z_0/2$. The characteristic impedance of the quarter-wave lines must be equal to $\sqrt{2}Z_0$ so that the input is matched when ports 2 and 3 are terminated in Z_0 .

The scattering parameters for the common case of a 2-way equal-split Wilkinson power divider at the design frequency is given by [8]

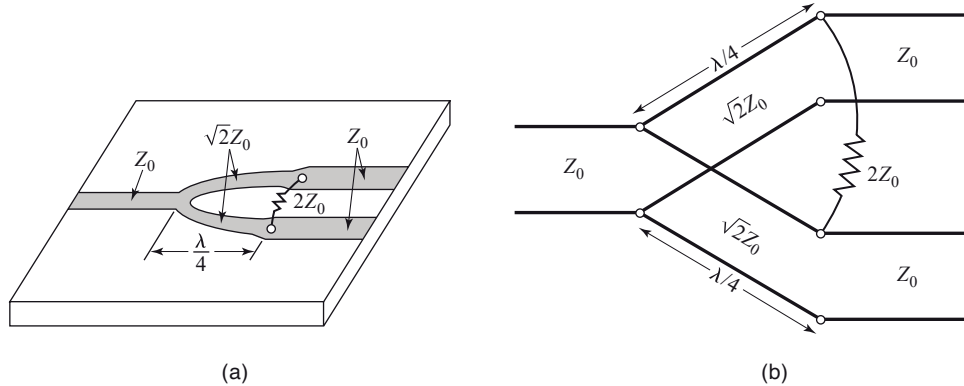
$$[S_{ij}] = \begin{bmatrix} 0 & 1 & 1 \\ 1 & 0 & 0 \\ 1 & 0 & 0 \end{bmatrix} \quad (5.1)$$

From the S matrix we see that the network is reciprocal ($S_{ij} = S_{ji}$), the terminals are matched ($S_{11}, S_{22}, S_{33} = 0$), the output terminals are isolated ($S_{23}, S_{32} = 0$), and the equal

¹The Wilkinson power splitter was invented around 1960 by an engineer named Ernes Wilkinson.

²It can be used also to combine two equal-phase signal into one in the opposite direction

Figure 5.9: The Wilkinson power divider. (a) An equal-split Wilkinson power divider in microstrip form. (b) Equivalent transmission line circuit.



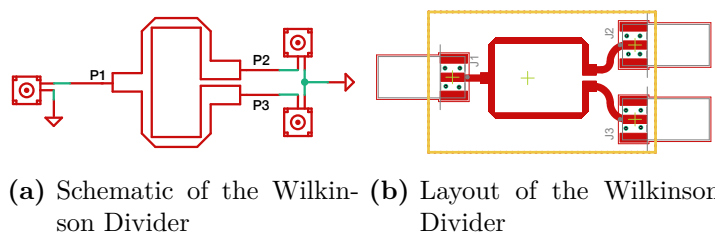
power division is achieved ($S_{21} = S_{31}$). As stated above, the Wilkinson splits the input power into two equal output power, this would be the ideal case, but since the networks are lossy this is not possible.³

5.4.2. Design procedure

The design of the Wilkinson Divider was done using the ADS Keysight software but unfortunately all the has been lost.

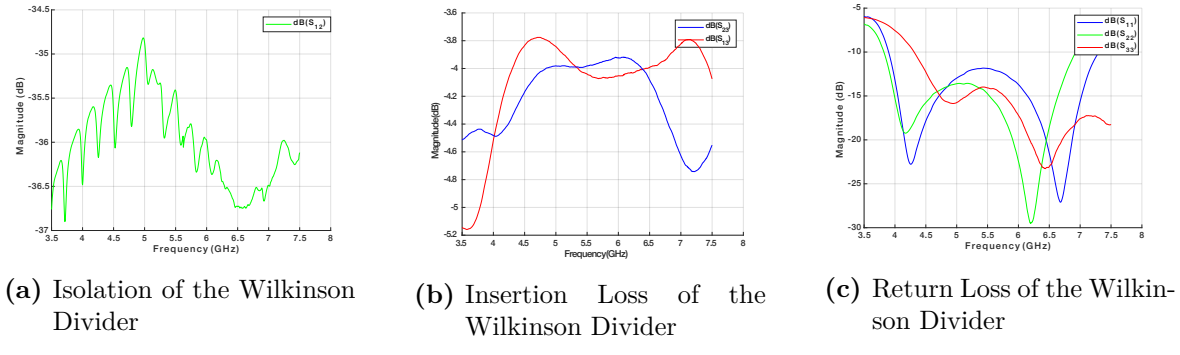
5.4.3. Experimental Results

The manufactured board is shown below



It is observed from the schematic simulation that the lumped model of the Wilkinson power divider has an insertion loss (S_{12} and S_{13}) of approximately 4 dB and return loss (S_{11}) of < 15 dB. The isolation is approximately -35dB.

³There is possible to make an unequal/asymmetric division through Wilkinson divider, but that its not the case.



5.5. Vivaldi Design

5.5.1. Introduction

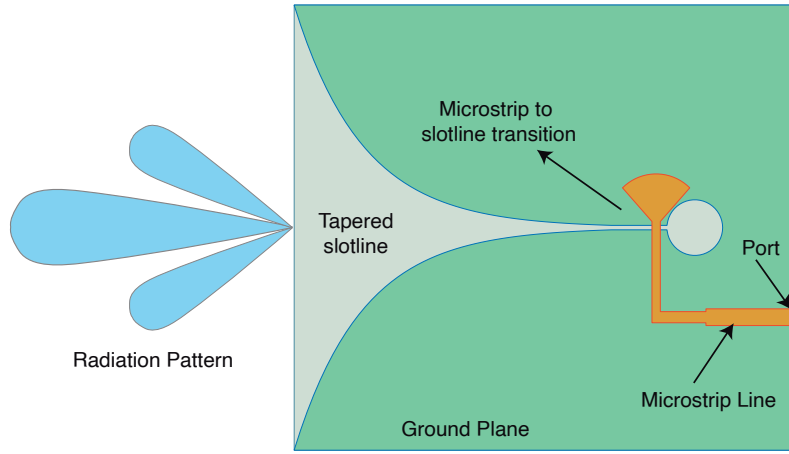
The Vivaldi antenna was designed following an example provided by Matlab [9] and the following paper [10]. The design model and analyze a vivaldi antenna with an internal matching circuit. The vivaldi is also known as an exponentially (. s are used in applications where is needed an Ultrawide bandwidth and was first introduced by P.J. Gibson in 1979 [11].

The configuration of the Vivaldi gives to it wideband characteristics, low cross polarization and a highly directive pattern. In general, [12] it has an end-fire radiation pattern, making it a member of the class of the continuously scaled, gradually curved, slow leaky end-fire traveling-wave-type antennas. At different frequencies, different parts of the Vivaldi antenna radiate, while the size of the radiating part is constant in wavelength. As such, the Vivaldi antenna has theoretically unlimited operating frequency. The design is implemented on a single layer dielectric substrate with 2 layers of metal; one for a flared slot line, and the feed line with the matching circuit on the other layer. The substrate is chosen as a low cost FR4 material of thickness 0.8 mm. The design is intended for operation over the frequency band 3.1 - 10.6 GHz. Finally the gerbers obtained with matlab were modified with the aid of the ADS Keysight.

5.5.2. Antenna design and configuration

The geometrical configuration of the proposed antenna is shown in Fig. 5.16. The antenna was designed in a substrate with a thickness of 0.8 mm, permittivity $\epsilon_r = 4.4$ and size of $45 \times 40 \text{ mm}^2$. The proposed Vivaldi antenna consist of a [10] microstrip feed line, microstrip line to slot line transition, and the radiating structure. Radiating structure is exponential tapered and the radiation takes place along the axis of the tapering. The continuous scaling and gradual curvature of the radiating structure ensures theoretically unlimited bandwidth [11].

Figure 5.12: This diagram demonstrates the configuration of the designed Vivaldi antenna



The tapered profile of the antenna is given by,

$$y(x) = ce^{K_a x} \quad (5.2)$$

where, constant c and opening rate K_a is given by

$$K_a = \frac{1}{L_a} \ln \left(\frac{W_a}{s} \right) \quad (5.3)$$

where, L_a , W_a , and S are the aperture length, the aperture width, and width of slot at origin.

Figure 5.13: Geometry of the proposed vivaldi antennas, (a) top view of antenna, (b) bottom view of antenna

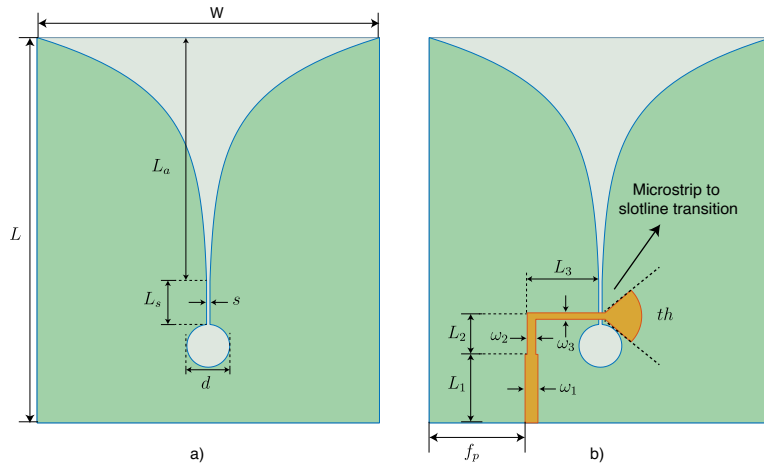


Table 5.1: Design parameters of the proposed antenna

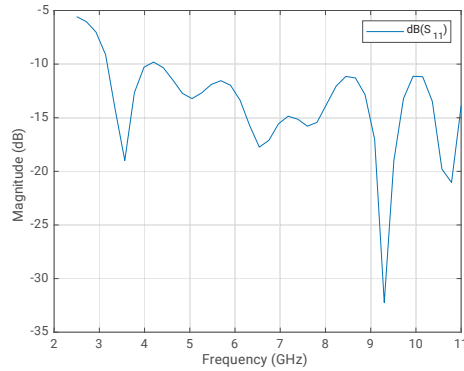
Parameter	L	W	L_s	L_a	W_a	s	d	$(^*)K_a$	L_1	L_2	L_3	W_1	W_2
Dimension (mm) ⁽¹⁾	45	40	5	28.5	39.9	0.4	5	161.5 m^{-1}	8	4.1	9.1	1.5	1

¹ Except (*)

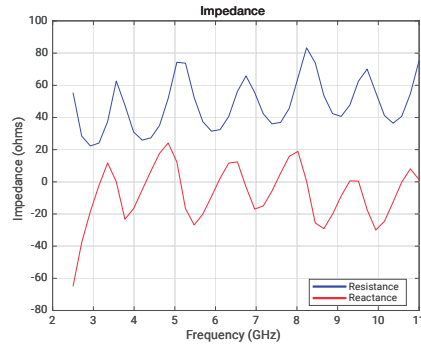
5.5.3. Simulation results and discussion

A. Reflection Coefficient

The variation of the reflection coefficient (S_{11}) with frequency are shown in Fig. 5.14. It is observed that the reflection coefficient is below -10 dB from 3.1 GHz to more than 11 GHz.

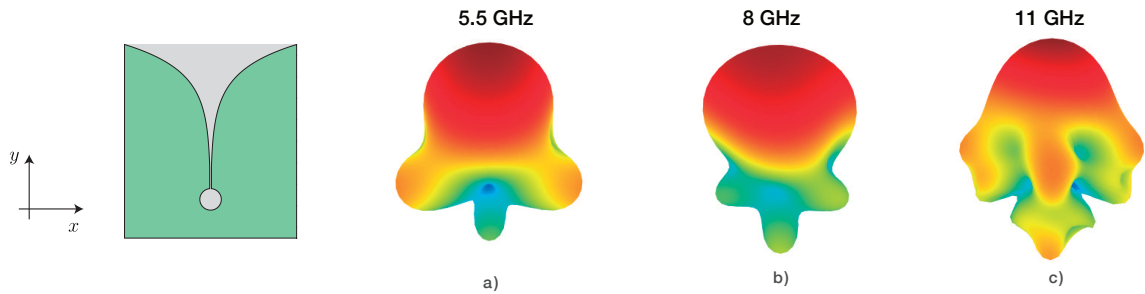
Figure 5.14: Reflection coefficient

B. Input Impedance

Figure 5.15: Impedance variation with frequency

The results of the input impedance are shown in Fig. 5.15. It is noted that the real and imaginary part of impedance is oscillating about 50Ω and 0Ω with frequency respectively. This results in matching with 50Ω SMA (Sub Miniature A) connector used to feed the antennas and wide impedance matching is achieved through microstrip to slotline transition.

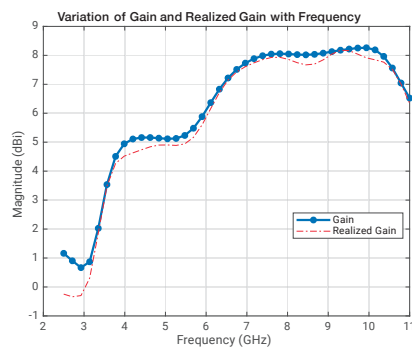
Figure 5.16: Radiation pattern of the antenna vivaldi at different frequencies.



C. Realized Gain

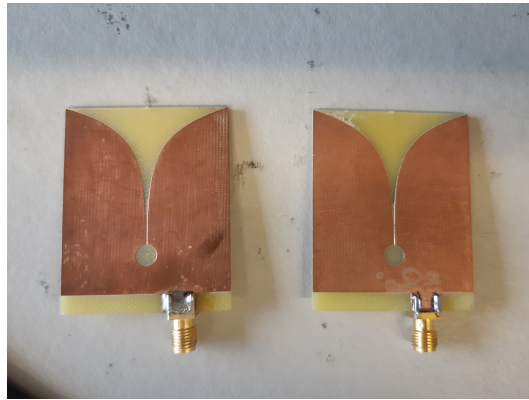
The variation of the realized gain is shown in Fig. 5.17. Its seen that at the 5.25 GHz the realized gain is about 5 dB . Finally, the wide impedance bandwidth characteristics of this antenna does not necessarily translate to a wide gain/pattern bandwidth. The highest gain is achieved over the $7 - 10.4\text{ GHz}$ range at boresight of approximately 9.5 dBi .

Figure 5.17: Gain variation with frequency

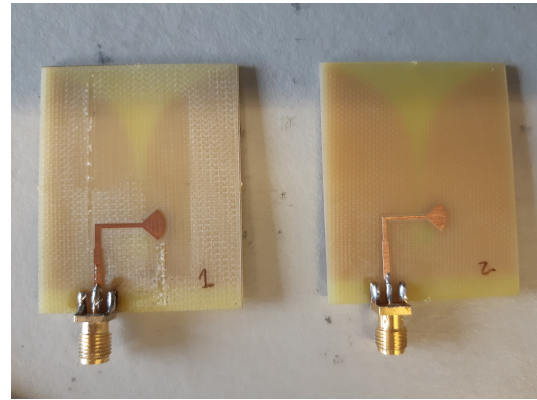


5.5.4. Experimental results

Two of the three fabricated antennas are shown in Fig 5.18a and 5.18b. The substrate is chosen as a low cost FR4 material of thickness 1.2 mm . This was an error since the simulation was done with a thickness of 0.8 mm . The third antenna was fabricated with a thickness of 0.8 mm and we see in Fig 5.19. For this antenna the experimental data fits better with the simulation.

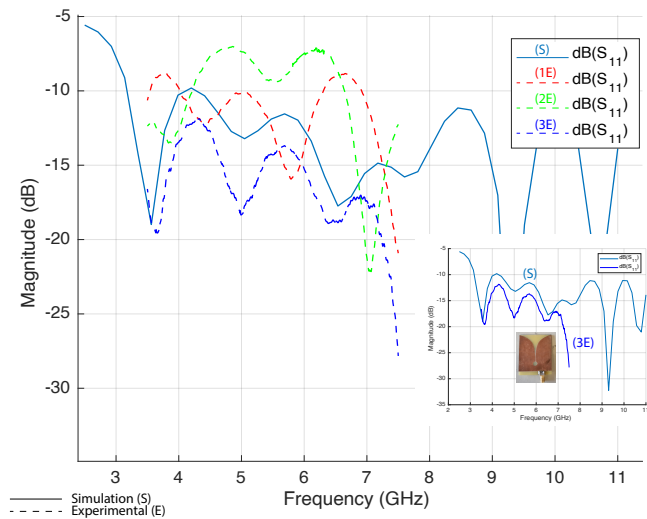


(a) Top view of the two antennas



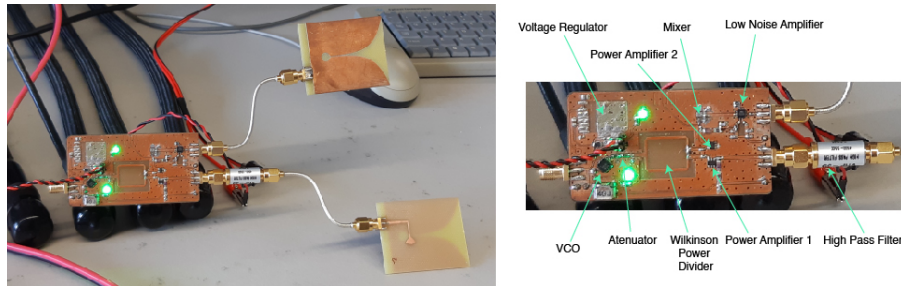
(b) Bottom view of the two antennas

As we can see in Fig 5.19 the reflection coefficient at the input relative to 50-ohm reference impedance is below -10 dB for the frequency range from 3.1 GHz to 11 GHz.

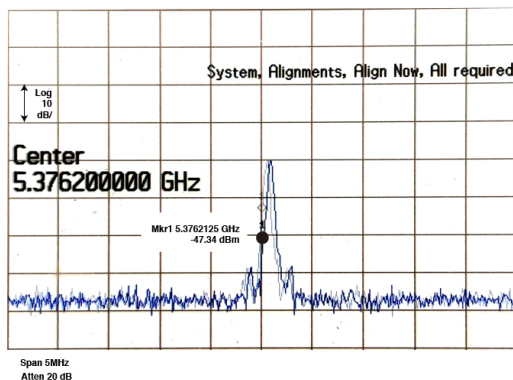
Figure 5.19: Comparasion of the simulation with the experimental results

5.6. Radar Results

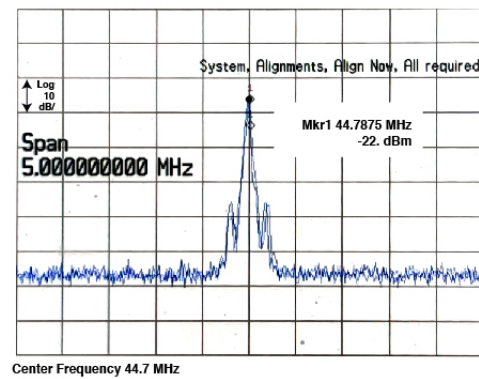
The radar test board is the last step of the test phase. As shown in previous sections a modular test approach is followed to verify that every component of the radar works as expected. In Fig 5.20 is shown the final PCB of the radar system. In this stage it was encountered that the footprint of the VCO was not correct. Due to this the test applied to the radar was difficult and hence the results are poor.

Figure 5.20: Radar board with the two antennas attached

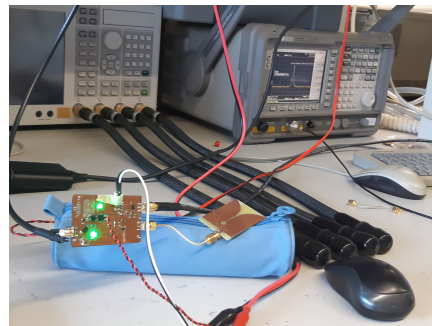
The output of the Mixer is shown in Fig 5.21b. As is shown the baseband spectrum is centered approximately at 44MHz and it has -22dB of power. This signal was acquired directly with the aid of an active probe at the output of the Mixer. The signal that was being sent with transmitter antenna is shown in Fig 5.21a.



(a) Spectrum of the output signal before going to the transmitter antenna



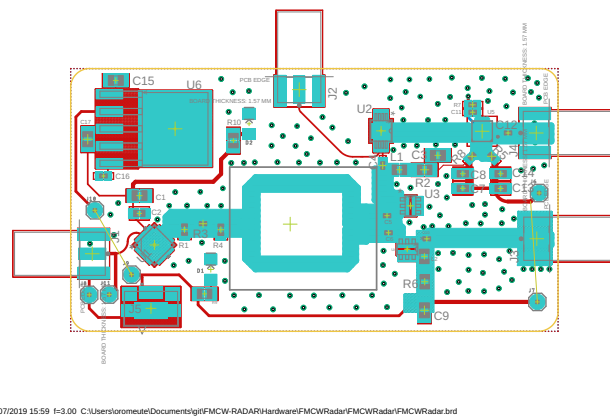
(b) Spectrum of the output of the mixer

Figure 5.22: Lab setup to test the FMCW Radar

5.7. Radar Revisited

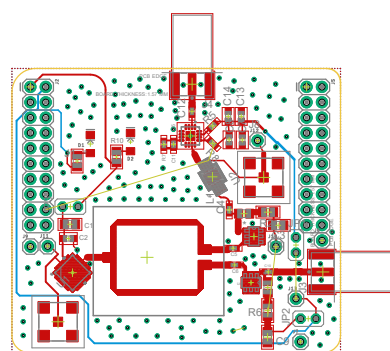
This chapter finishes with the PCB layout of the modified version of the radar. This version of the radar solved the problem with VCO footprint. The initial board layout is shown below

Figure 5.23: Initial FMCW Radar Layout



Also, it was followed the design guidelines to work with TI-Launchpad ecosystem. The idea is to process the baseband signal with an MSP432 Launcpad.

Figure 5.24: Modified PCB layout of the initial FMCW Radar.



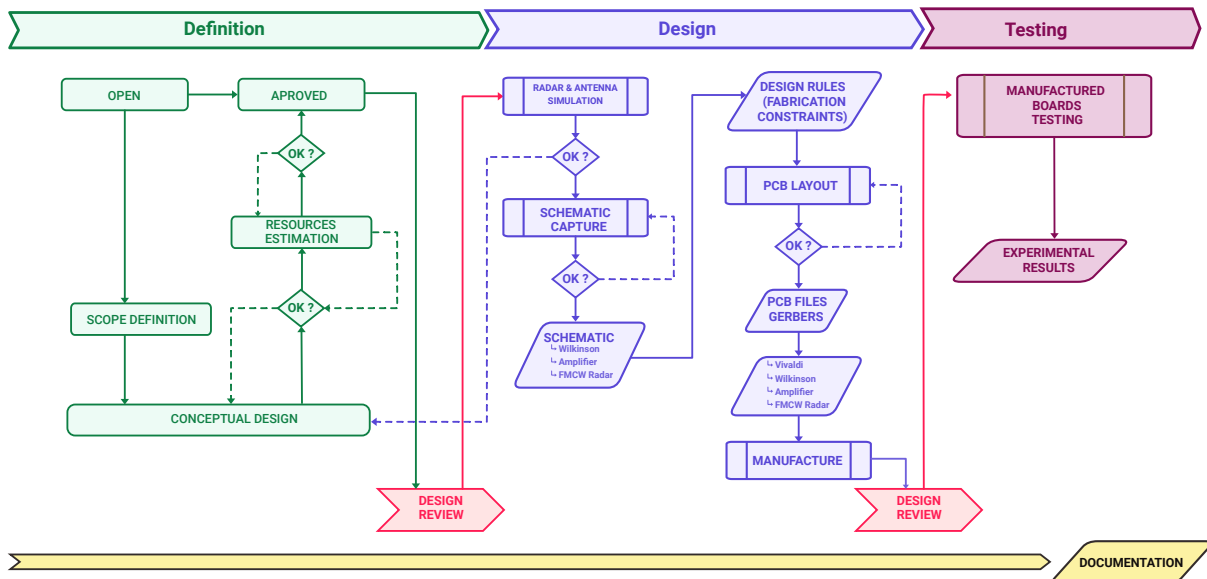
Finally, the schematics are shown in the appendix section.

6. Feasibility study of the project

6.1. Execution planning

The project was done following a continuous testing approach. The first step of any hardware project is to state the scope of the project that is the main product application — where it'll be used, how and by whom and what include. After that we have modeled the scope in a conceptual design which will serve to us as a guide to make an estimation of the resources that are needed to make a prototype. These ideas are summarized in the Fig. 6.1

Figure 6.1: Flow diagram of the project



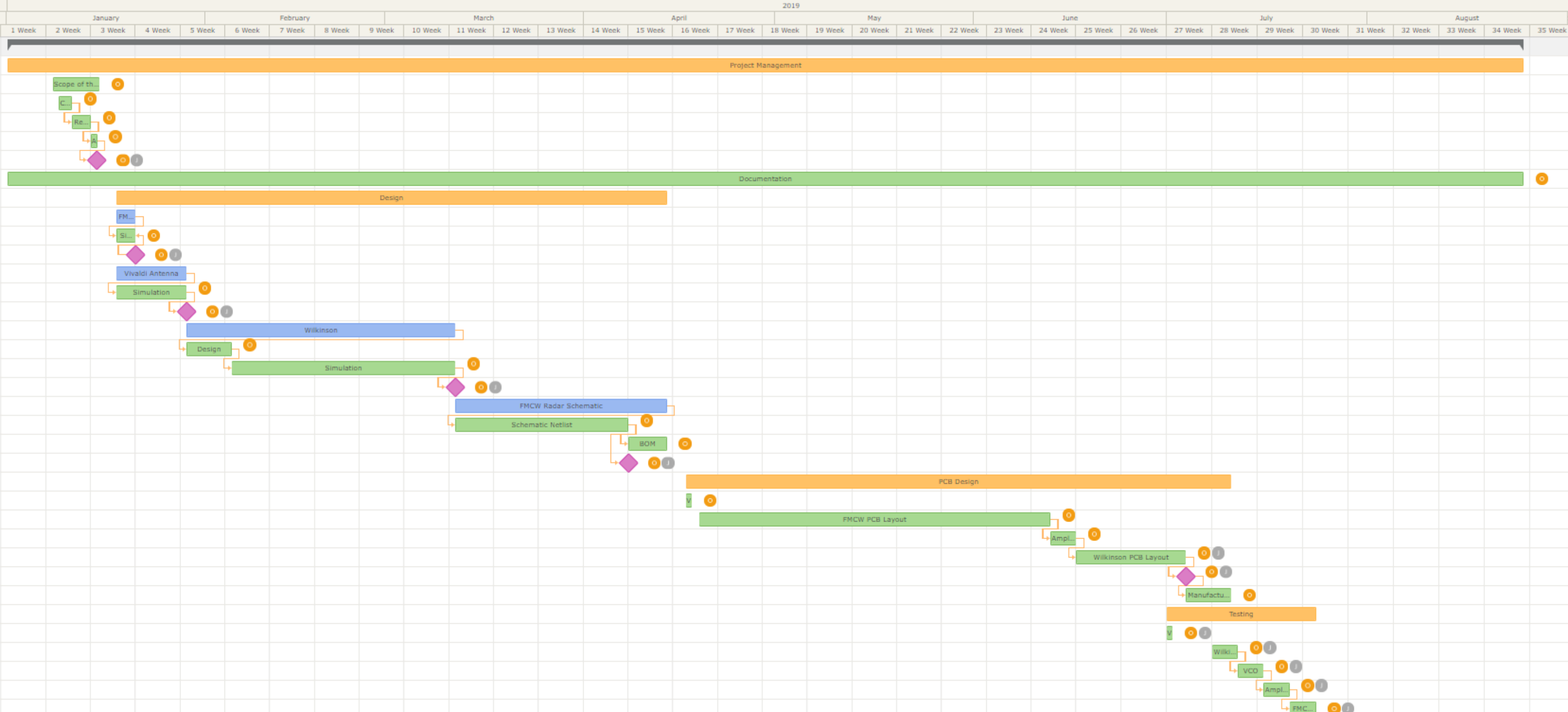
The second step was a proof of concept (POC). Working in uncharted territory serve to test the conceptual design and the technologies used. In this step it is important to modularize as much as possible the model because in that way is easier to made a troubleshooting. In this step a simulation of the radar, Wilkinson splitter and the antenna is made. Finally, the PCB of the radar, amplifier and the antennas.

The third and the last step is to sent to the manufacturer the gerber files and get the PCBs

to test it. Since this project was done at the university we used the facilities provided at the faculty of to made the prototypes. In Fig ?? we have and the Workbench structure and the Gantt diagram of the project is shown in the next page.

		Task name	Assigned	Start date	End date	Estimation (hours)
1		Project Management		2019/01/01	2019/08/25	11313h
1.1		Scope of the project	Oscar Romeu	2019/01/08	2019/01/15	177h
1.2		Conceptual Design	Oscar Romeu	2019/01/09	2019/01/11	48h
1.3		Requirements & Constraints	Oscar Romeu	2019/01/11	2019/01/14	72h
1.4		Aprove	Oscar Romeu	2019/01/14	2019/01/15	24h
1.5		Validation	O J	2019/01/15	2019/01/15	
1.6		Documentation	Oscar Romeu	2019/01/01	2019/08/25	5664h
2		Design		2019/01/17	2019/04/14	2136h
2.1		FMCW Radar Architecture		2019/01/18	2019/01/21	72h
2.1.1		Simulation	Oscar Romeu	2019/01/18	2019/01/21	72h
2.1.2		Validation	O J	2019/01/21	2019/01/21	
2.2		Vivaldi Antenna		2019/01/17	2019/01/28	264h
2.2.1		Simulation	Oscar Romeu	2019/01/17	2019/01/28	264h
2.2.2		Validation	O J	2019/01/28	2019/01/28	
2.3		Wilkinson		2019/01/28	2019/03/11	1008h
2.3.1		Design	Oscar Romeu	2019/01/28	2019/02/04	168h
2.3.2		Simulation	Oscar Romeu	2019/02/04	2019/03/11	840h
2.3.3		Validation	O J	2019/03/11	2019/03/11	
2.4		FMCW Radar Schematic		2019/03/12	2019/04/14	792h
2.4.1		Schematic Netlist	Oscar Romeu	2019/03/12	2019/04/08	648h
2.4.2		BOM	Oscar Romeu	2019/04/08	2019/04/14	144h
2.5		Validation	O J	2019/04/08	2019/04/08	
3		PCB Design		2019/04/17	2019/07/11	2424h
3.1		Vivaldi Gerbers	Oscar Romeu	2019/04/17	2019/04/18	24h
3.2		FMCW PCB Layout	Oscar Romeu	2019/04/19	2019/06/13	1320h
3.3		Amplifier PCB Layout	Oscar Romeu	2019/06/13	2019/06/17	96h
3.4		Wilkinson PCB Layout	O J	2019/06/17	2019/07/04	816h
3.5		Validation	O J	2019/07/04	2019/07/04	
3.6		Manufactured	Oscar Romeu	2019/07/04	2019/07/11	168h
4		Testing		2019/07/01	2019/07/24	768h
4.1		Vivaldi	O J	2019/07/01	2019/07/02	0
4.2		Wilkinson	O J	2019/07/08	2019/07/12	192h
4.3		VCO	O J	2019/07/12	2019/07/16	192h
4.4		Amplifier	O J	2019/07/16	2019/07/20	192h
4.5		FMCW RadarPCB	O J	2019/07/20	2019/07/24	192h

Figure 6.2: Workbench structure of the project.



6.2. Economical aspects

The total cost of the radar is show in Table 6.1

Table 6.1: Bill of materials of the FMCW radar

Vendor	Vendor No	Mfr. No	Manufacturer	Description	Order Qty.	Price (EUR)	Ext.: (EUR)
Mouse							
1	80-C0402C103K-4R7867	C0402C103K4RAC7867	KEMET	Multilayer Ceramic Capacitors MLCC - SMD/SMT 16V 0.01nF X7R 0402 10%	40	0.015	0.6
2	80-C0603C102J5RAUTO	C0603C102J5RAUTO	KEMET	Multilayer Ceramic Capacitors MLCC - SMD/SMT 50V 1000pF 0603 X7R 5% AEC-Q200	20	0.038	0.76
3	667-ERJ-2RKF5761X	ERJ-2RKF5761X	Panasonic	Thick Film Resistors - SMD 0402 5.7kOhms 1% AEC-Q200	10	0.039	0.39
4	755-SFR01M2P1000	SFR01M2P1000	ROHM Semiconductor	Thick Film Resistors - SMD 0402 Jumper 5% Anti-Sulfur AEC-Q200	20	0.056	1.12
5	667-ERJ-2RKF17R8X	ERJ-2RKF17R8X	Panasonic	Thick Film Resistors - SMD 0402 17.5ohms 1% AEC-Q200	3	0.087	0.26
6	74-T58W0475M025C0500	T58W0475M025C0500	Vishay	Tantalum Capacitors - Polymer SMD 4.7uF 25volts 20% 500mohms maxESR	5	0.856	4.28
7	80-C0603C103KARACAUTO	C0603C103KARACAUTO	KEMET	Multilayer Ceramic Capacitors MLCC - SMD/SMT 250V 0.01nF 0603 X7R 10% AEC-Q200	5	0.786	3.93
8	963-HK21253N3S-T	HK21253N3S-T	Taivo Yuden	Fixed Inductors 0805 3.3nH 130mOhms +/-5% Tol 300mA HiQ	10	0.154	1.54
9	603-C0402KR8BB101	CC0402KR8BB101	Yageo	Multilayer Ceramic Capacitors MLCC - SMD/SMT 100pF 25V 10% 0402 Case Size	10	0.017	0.17
10	755-KTR10EZP1220	KTR10EZP1220	ROHM Semiconductor	Thick Film Resistors - SMD 0805 22ohm 5% High Voltage	10	0.098	0.98
11	963-LMK212AB7225KD-T	LMK212AB7225KD-T	Taivo Yuden	Multilayer Ceramic Capacitors MLCC - SMD/SMT 10volts 2.2uF X7R 10% 0805 HiCV	10	0.138	1.38
12	474-BOB-12918	BOB-12918	SparkFun Electronics	Daughter Cards & OEM Boards I2C DAC Breakout - MCP4725	1	4.32	4.32
13	963-UMK105CG1R2BV-F	UMK105CG1R2BV-F	Taivo Yuden	Multilayer Ceramic Capacitors MLCC - SMD/SMT 0402 50VDC 1.2pF C0G Tol 0.1pF Gen Purp	10	0.021	0.21
14	80-C0603X104J5R3190	C0603X104J5RAC3190	KEMET	Multilayer Ceramic Capacitors MLCC - SMD/SMT 50V 0.1nF 0603 X7R 5% AEC-Q200	10	0.348	3.48
15	660-RNT31JTD2910D100	RNT31JTD2910D100	KOA Speer	Thin Film Resistors - SMD 2910Ohm,06030.3%,10p .pm.63mW,50V	10	0.201	2.01
16	595-BOOSTXL-BATPAKMKII	BOOSTXL-BATPAKMKII	Texas Instruments	Multiple Function Sensor Development Tools BOOSTXL-BATPAKMKII	1	24.96	24.96
Digikey							
1	1127-1385-1-ND	HMC430LP4ETR	Analog Devices	IC MMIC VCO HBT W/BUFFER 24-QFN	2	17.240	34
2	1127-3400-ND	HMC717ALP3E	Analog Devices	IC RF AMP LTE 4.5GHZ-6GHZ 16QFN	2	11	22
3	1127-2873-ND	HMC218BMS8GE	Analog Devices	IC MMIC MIXER DBL-BAL 8MSOP	2	6	12
4	1127-3509-ND	HMC313	Analog Devices	IC RF AMP WLAN 0HZ-6GHZ SOT26	5	4	20
Total						113.070	
Total						137.430	

7. Conclusions and future work

The FMCW radar project is a very exciting project but it has many difficulties. First of all, it is a project that requires a long time since many tasks have to be done in order to build a prototype. Ideally, you should start with a modular approach, test all the modules separately and then join them in a final design. To carry out this project ideally it should be done between three people in this way the signal processing part could be included.

This chapter finishes with a summarized ideas of future work

- Change the Wilkinson Divider for Coupler divider design. This could give us the flexibility to redistribute the power.
- A 4 layer layout design is better option to design the radar since this way we separate the signal layer with power and ground layer.
- Process the IF signal with the aid of a microcontroller. Before processing the signal with a microcontroller a base band signal board has to be done in order to accomodate the signa to the input ADC of the microcontroller.

Bibliography

- [1] wikipedia. (2019, aug) Relativistic doppler effect. [Online]. Available: https://en.wikipedia.org/wiki/Relativistic_Doppler_effect
- [2] E. M. i Soler, *Curs de relativitat especial*, 2nd ed. Universitat Autònoma de Barcelona, 1998.
- [3] I. T. Union, “Rr2016vol-i-ea5,” *Radio Regulation Articles*, 2016.
- [4] G. L. Charvat, A. J. Fenn, and B. T. Perry, “The mit iap radar course: Build a small radar system capable of sensing range, doppler, and synthetic aperture (sar) imaging,” in *2012 IEEE Radar Conference*, May 2012, pp. 0138–0144.
- [5] N. K. Samuel Wagner, Andy Chen. (2017, apr) The design and implementation of a fmcw radar system. [Online]. Available: http://dart.ece.ucdavis.edu/education/files/eec134-2016-2017/Team_WCKSS/Team_WCKSS_Report.pdf
- [6] N. Klein. (2017, jan) Designing a custom antenna. [Online]. Available: http://dart.ece.ucdavis.edu/education/files/eec134-2016-2017/Team_WCKSS/AN_Natalie_Killeen_+.pdf
- [7] wikipedia. (2019, jun) Vivaldi antenna. [Online]. Available: https://en.wikipedia.org/wiki/Vivaldi_antenna
- [8] D. M. Pozar, *Microwave Engineering*, 2nd ed. John Wiley & Sons, 1998.
- [9] MathWorks. (accessed July 22, 2019) Design an internally matched ultra-wideband vivaldi antenna. [Online]. Available: <https://es.mathworks.com/help/antenna/examples/design-an-internally-matched-ultra-wideband-vivaldi-antenna.html>
- [10] G. Pandey, H. Singh, P. Bharti, A. Pandey, and M. Meshram, “High gain vivaldi antenna for radar and microwave imaging applications,” *International Journal of Signal Processing Systems*, vol. 3, 01 2014.
- [11] P. J. Gibson, “The vivaldi aerial,” in *1979 9th European Microwave Conference*, Sep. 1979, pp. 101–105.
- [12] M. N. Dr. J.S. Mandep. (accessed July 31, 2019) Design an x-band vivaldi antenna. [Online]. Available: <https://www.mwrf.com/markets/design-x-band-vivaldi-antenna>

- [13] H.D.Griffiths, "New ideas in FM radar," *Electronics & Communication Engineering Journal*, Oct. 1990.
- [14] A.G.Stove, "Linear FMCW radar techniques," *IEE Proceedings F - Radar and Signal Processing*, vol. 139, pp. 343 – 350, Oct. 1992.

A. Datasheets

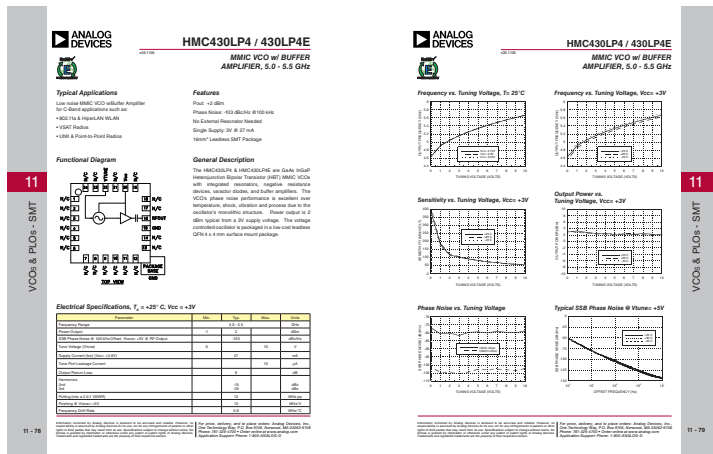
A.1. Mixer

Figure A.1: <https://www.analog.com/media/en/technical-documentation/data-sheets/hmc218b.pdf>



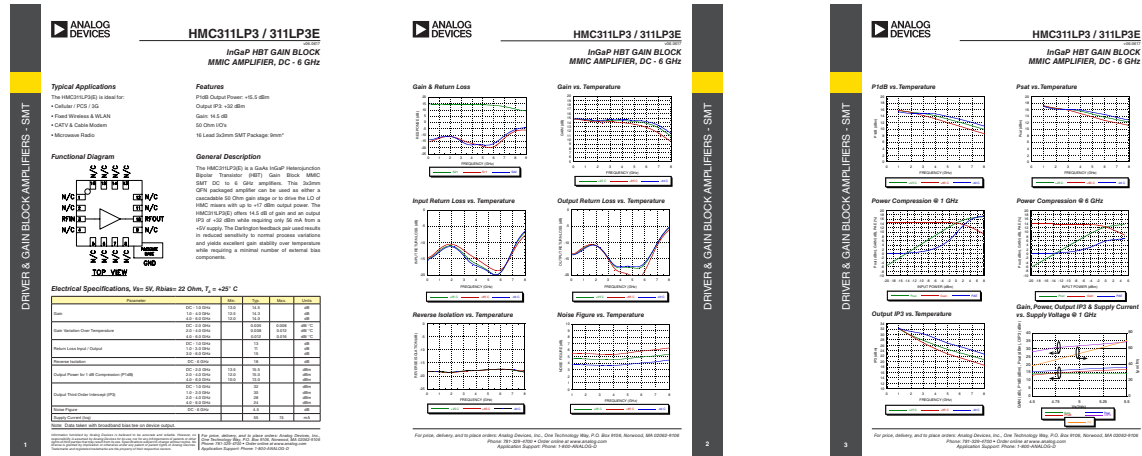
A.2. Voltage Controlled Oscillator

Figure A.3: <https://www.analog.com/media/en/technical-documentation/data-sheets/hmc430.pdf>



A.3. Power Amplifier

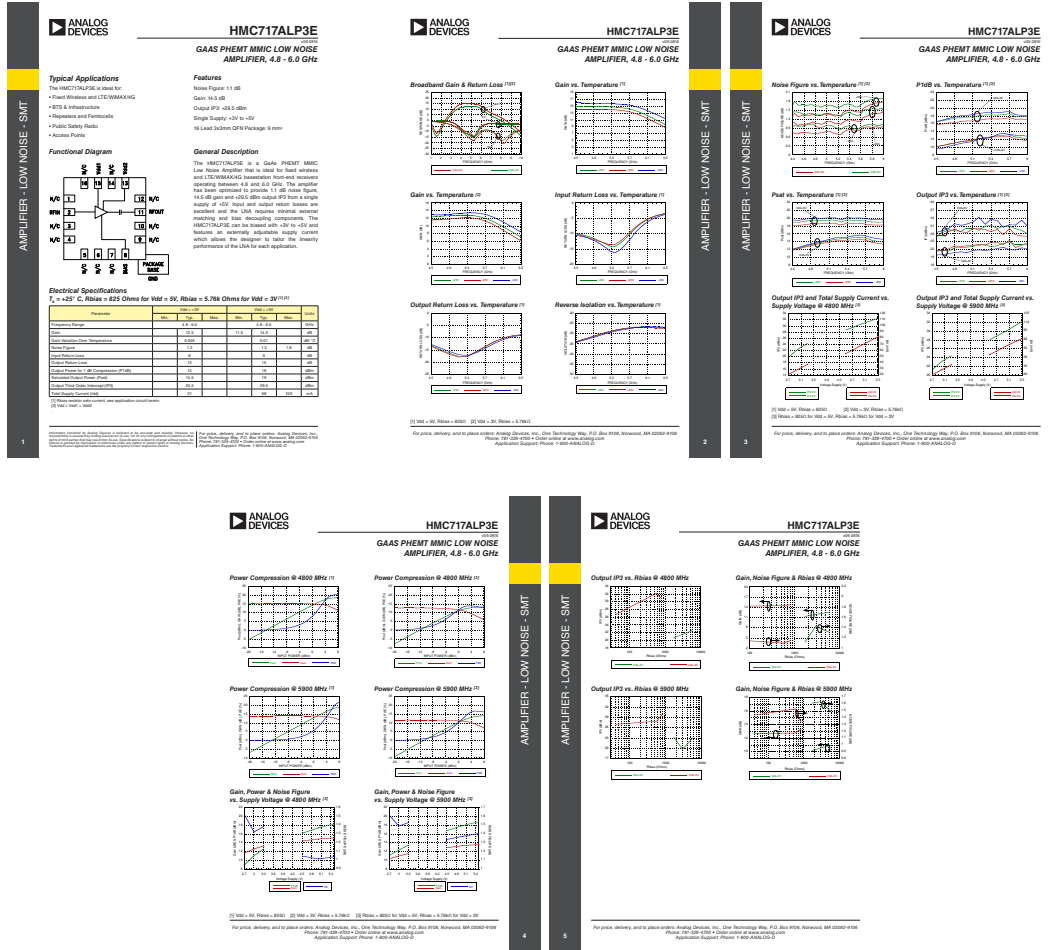
Figure A.5: <https://www.analog.com/media/en/technical-documentation/data-sheets/hmc311lp3.pdf>



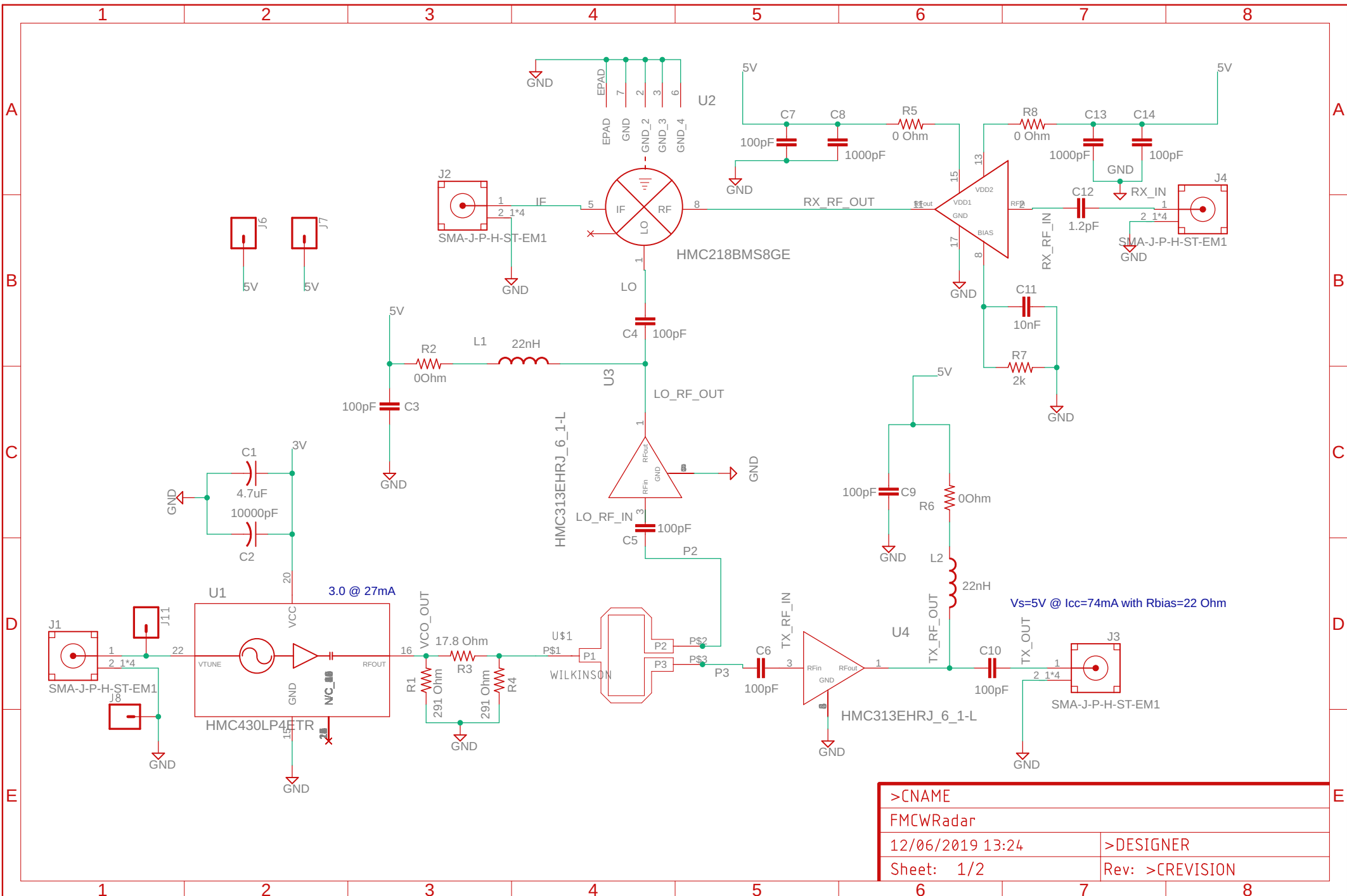
A.4. LOW NOISE AMPLIFIER

A.4. Low Noise Amplifier

Figure A.7: <https://www.analog.com/media/en/technical-documentation/data-sheets/hmc717a.pdf>



B. Schematics



1 2 3 4 5 6 7 8

A

B

C

D

E

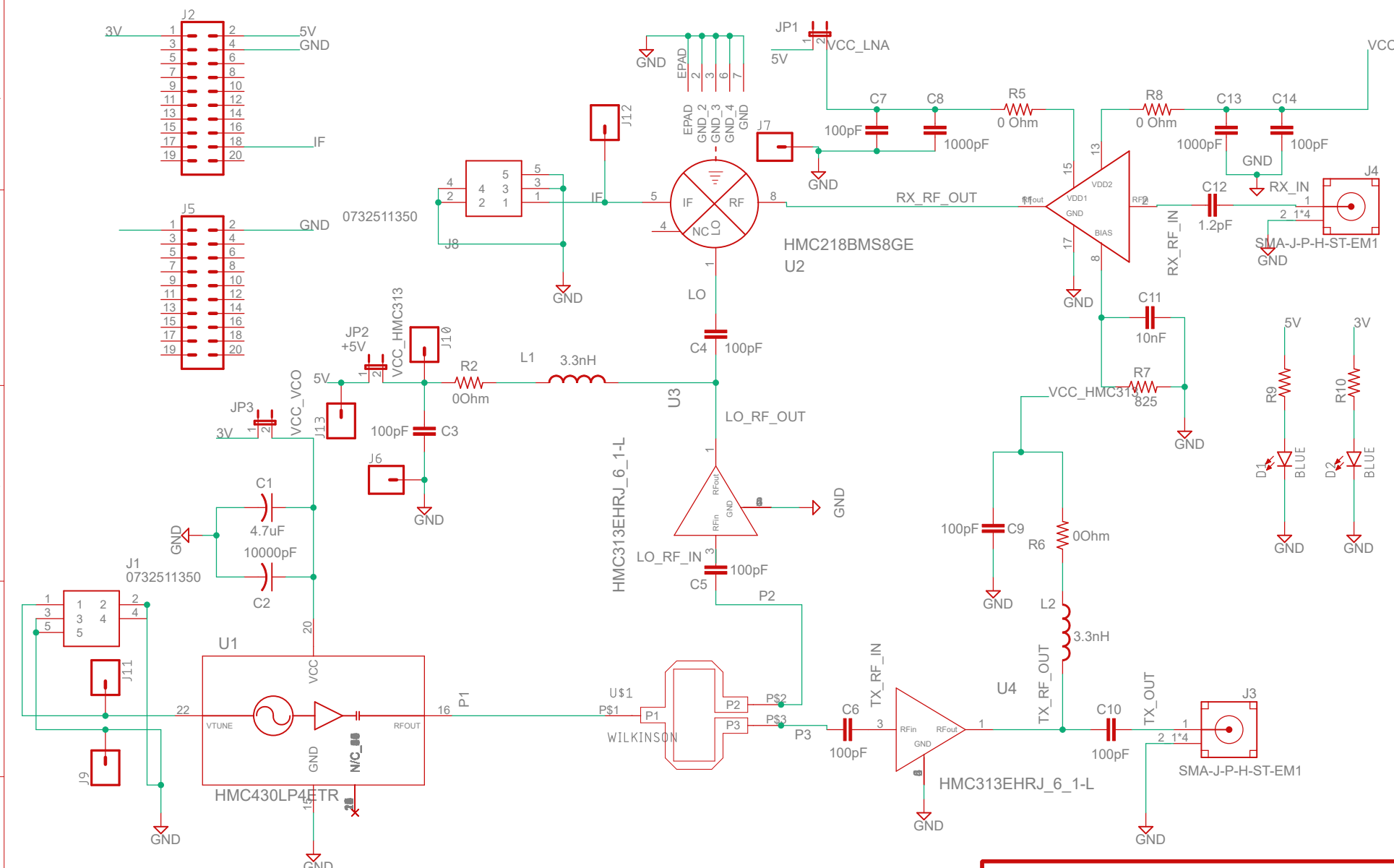
A

B

C

D

E



Bachelor Thesis

FMCWRadarv2

24/8/19 16:39

Sheet: 1/1

Oscar Romeu

Rev: